Published November 8, 2010

INAM-expressing stable BaF3 cell lines (INAM/BaF3) did not reveal a function as an NK cell–activating ligand. NK cell cytotoxicity is directed against Rae-1α/BaF3 cells but not against INAM/BaF3 cells (Fig. 5). Therefore, INAM does not represent a typical NK cell–activating ligand. For NK activation, INAM on BMDC appears to require other molecules that are expressed in BMDC but not in BaF3.

INAM has four transmembrane regions, similar to the cell adhesion tetraspanins, which may support cell–cell contact (Levy and Shoham, 2005). Tetraspanins provide a scaffold that facilitates complex formation with associated proteins. INAM on BMDC and NK cells may use cell–cell interaction to assemble in a synaptic formation to activate NK cells. Because the protein constituents of the tetraspanin complexes are cell specific, we are interested in finding partners for INAM that might participate in efficient BMDC–NK interaction. TLR-inducible cell–cell contact may occur through INAM in an immune cell–specific manner. Gene disruption of this INAM will facilitate clarifying this issue. The identification of INAM defines a novel pathway in mDC–NK reciprocal interaction. This study will lead to further research on the molecules that form complexes on BMDC and NK cells to facilitate BMDC–NK interaction.

MATERIALS AND METHODS

Mice. All mice were backcrossed with C57BL/6 mice more then seven times before use. TICAM-1$^{-/-}$ (Akazawa et al., 2007a) and IPS-1$^{-/-}$ mice were generated in our laboratory. IRF-3$^{-/-}$ (Sato et al., 2000) and IRF-7$^{-/-}$ mice (Honda et al., 2005) were provided by T. Taniguchi (University of Tokyo, Tokyo, Japan). All mice were maintained under specific pathogen-free conditions in the animal facility of the Hokkaido University Graduate School of Medicine. Animal experiments protocols and guidelines were approved by the Animal Safety Center, Hokkaido University, Japan.

Cells. The B16D8 cell line was established in our laboratory as a subline of B16 melanoma (Tanaka et al., 1988). This subline was characterized by its low or virtually no metastatic properties when injected s.c. into syngeneic C57BL/6 mice. B16D8 was cultured in RPMI 1640/10% FCS. The mouse B cell line BaF3 was obtained from American Type Culture Collection and cultured in RPMI 1640/10% FCS/2 μM 2ME/5 ng/ml IL-3. Mouse NK cells (DX5^{+} cell) were positively isolated with MACS Beads (Miltenyi Biotec). Mouse BMDCs were prepared as previously reported (Akazawa et al., 2007a).

For purification of cells from spleen or LN, these tissues were treated with 400 IU MandleU/ml collagenase D (Roche) at 37°C for 25 min in HBSS (Sigma-Aldrich). Then EDTA was added, and the cell suspension was incubated for an additional 5 min at 37°C. After removal of RBC with ACK lysis buffer, splenocytes and LN cells were stained with CD45-FITC, CD3ε-PE, CD19-PE, DX5-PE, CD11b-FITC (eBioscience), and CD11c-FITC (BioLegend) and sorted by a FACSAria II (BD). The purity of sorted cells were >96%.

Construction and expression. Mouse INAM cDNA (A630077B13Rik) was obtained from RIKEN and placed into expression vector pEFBOS and pLenti-IRES-hrGFP, both of which provide the specialized components needed for expression of a recombinant C-terminal FLAG fusion (Akazawa et al., 2007a). For construction of shRNA-expressing lentivirus vector, The ClaI–XhoI fragment of pLenti6-blockit-dest (Invitrogen) was inserted into pLenti-IRES-hrGFP at the site of ClaI and XhoI. This vector was named pLenti-dest-IRES-hrGFP (pLDIG). INAM sequence 5′-CTTCTCTCCG-GTTAGTTATCT-3′ was targeted for INAM knockdown (shINAM/pLDIG) and 5′-AGTCTGACATACTTATACTTA-3′ was used for negative control (shCont/pLDIG). We used a gene-expression kit, Lentiviral system (Invitrogen), as previously described (Akazawa et al., 2007a). Four plasmids (one of the pLenti vectors, pLP1, pLP2, and pLP/VSVG) were transfected into 293 FT packaging cells, and the viral particles for transfection were prepared according to the manufacturer's protocol. The 100× concentrated virus particles were produced after centrifugation of 8,000 *g* at 4°C for 16 h. Lentivirus produced by pLenti-IRES-hrGFP and pLDIBG could be tittered by GFP expression using flow cytometry. Because the lentivirus vector pLenti-IRES-hrGFP has the IRES-GFP region, we prepared negative control virus by pLenti-IRES-hrGFP without construct. Infection efficiency for BMDC was high with the control vector compared with the INAM-expressing lentivector (Fig. S6 A).

Real-time PCR. BMDCs were harvested after 4 h of stimulation by 100 ng/ml LPS, 50 μg/ml polyI:C, 1 μg/ml Pam_3CSK_4 (Pam3), 100 nM mycoplasmal macrophage-activating lipopeptide-2 (Malp-2), 10 μg/ml CpG, and 2,000 IU/ml IFN-α (Ebihara et al., 2007). Mouse tissues (heart, stomach, small intestine, large intestine, lung, brain, muscle, liver, kidney, thymus, and spleen) were collected from C57BL/6. Splenocytes were stained with CD3-PE, CD19-PE, DX5-PE, CD11b-PE, CD11c-FITC, and PDCA1-PE (eBioscience) and sorted by FACSAria (BD). Purity was >98% in each population. For RNA extraction, we used the RNeasy kit (Invitrogen). After removal of genomic DNA by treatment with DNase, randomly primed cDNA strands were generated with Moloney mouse leukemia virus reverse transcription (Promega). RNA expression was quantified by quantitative RT-PCR with gene-specific primers (IL-15 forward, 5′-TTAACTGAGGCTGGCATTCATG-3′; IL-15 reverse, 5′-ACCTACACTGACACAGCCCAAA-3′; INAM forward, 5′-CAACTGCAATGCCACGCTA-3′; INAM reverse, 5′-TCCAACC-GAACACCTGAGACT-3′; β-actin forward, 5′-TTTGCAGCTCCTTC-GTTGC-3′; β-actin reverse, 5′-TCGTCATCCATGGCGAACT-3′; HPRT forward, 5′-GTTGGATACAGGCCAGACTTTGTTG-3′; and HPRT reverse, 5′-GAAGGGTAGGCTGGCCTATAGGCT-3′) and values were normalized to the expression of β-actin mRNA or HPRT mRNA.

Other primers for PCR were designed using Primer Express software (Applied Biosystems) for another experiment. The following primers were used for PCR: β-actin forward, 5′-CCTGGCACCCAGCACAAT-3′ and reverse, 5′-GCCGATCCACACGGAGTACT-3′; granzyme B forward, 5′-TCCTGCTACTGCTGACCTTGTC-3′ and reverse, 5′-ATGATCTC-CCCTGCCTTTGTC-3′; IFN-α4 forward, 5′-CTGCTGGCTGTGAG-GACATACT-3′ and reverse, 5′-AGGCACAGAGGCTGTGTTTCTT-3′; TRAIL (Tnfsf10) forward, 5′-CTTCACCAACGAGATGAAGCAG-3′ and reverse, 5′-TCCGTCTTTGAGAAGCAAGCTA-3′; and IL-12p40 (Il12b), forward, 5′-AATGTCTGCGTGCAAGCTCA-3′ and reverse, 5′-ATGCCCACTTGCTGCATGA-3′.

Anti-INAM pAb. C-terminal INAM (cINAM; 191–314 aa) was subcloned between the NdeI and SalI sites of pColdI vector (Takara Bio Inc.). 6× His-tagged cINAM protein was expressed in BL21 by manufacturer's methods. The cells were sonicated in 20 mM Tris-HCl, 150 mM NaCL, 1 mM PMSF, and 7 M Urea, pH 7.4, on ice. Expression products of cINAM were purified using the HisTrap HP kit (GE Healthcare). The extracted proteins were refolded by step-wise dialysis against decreasing amounts of urea. Rabbit anti-cINAM polyclonal Ab was produced with the cINAM proteins by standard protocol. IgG was purified by precipitation with 33% ammonium sulfate, dialyzed against PBS.

Surface labeling with biotin. Biotinylation of cell surface proteins was performed according to the reported method (Tsuji et al., 2001). In brief, ~10^8 cells were suspended in 1 ml Hepes-buffered saline (HBS), pH 8.5, and incubated with 10 ml of 10 mg/ml NHS-sulfobiotin (Vector Laboratories) for 1 h at room temperature. Cells were washed in HBS three times and then solubilized with lysis buffer containing 1% NP-40, pH 7.4. The cell lysate was immunoprecipitated with avidin-labeled Abs as described previously (Tsuji et al., 2001).

Immunoblot analysis. Lysates were harvested 24 h after transfection of Flag-tagged INAM/pEFBOS into 293FT cells and treated with *N*-glycosidase F

Downloaded from jem.rupress.org on November 24, 2010

(PNGaseF; New England Biolabs, Inc.) by the manufacturer's method in some experiments. Protein samples were separated on SDS-PAGE and immunoblotted by anti-Flag M2 Ab (Sigma-Aldrich). In some experiments, we used highly purified rabbit anti–mouse INAM polyclonal Ab for immunoblotting. The anti-INAM IgG was further purified with protein A–Sepharose and absorbed with BL21 bacterial lysate (where the INAM immunogen was produced) that contained no INAM peptide.

Confocal microscopy. BMDCs and NK cells were infected with control or INAM-expressing lentivirus as described previously (Akazawa et al., 2007a). 24 h later, cells were fixed with 4% paraformaldehyde for 30 min and permeabilized with PBS containing 0.5% saponin for 30 min at room temperature. Fixed cells were stained with anti-FLAG mAb and Alexa Fluor 568–conjugated secondary Ab. Stable Ba/F3 transfectants expressing INAM were treated with Cytofix/Cytoperm (BD) according to the manufacturer. Then cells were stained with PE-phalloidin and rabbit anti-INAM pAb followed by Alexa Fluor 488–conjugated secondary Ab. Cells were analyzed on a confocal microscope (LSM 510 META; Carl Zeiss, Inc.) for the detection of INAM.

BMDC–NK interaction. BMDCs were co-cultured with freshly isolated NK cells (BMDC/NK = ~1:2–1:5) with or without 10 μg/ml polyI:C for 24 h (Akazawa et al., 2007a). In some experiments, function of BMDCs and NK cells was modified by lentivirus vector before BMDC/NK co-culture. IRF-$3^{-/-}$ BMDCs were transfected by control lentivirus and INAM-expressing lentivirus (INAM/pLenti-IRES-hrGFP) and incubated with 6 μg/ml polybrene for 24 h before co-culture. WT BMDCs were transfected with shRNA-expressing lentivirus (shCont/pLDIG or shINAM/pLDIG) and incubated with 6 μg/ml polybrene for 48 h before co-culture. Freshly isolated NK cells were transfected with control lentivirus and INAM-expressing lentivirus (INAM/pLenti-IRES-hrGFP) and cultured with 6 μg/ml polybrene in the presence of 500 IU/ml IL-2 for 72 h before co-culture. Activation of NK cells was assessed by concentration of IFN-γ (ELISA; GE Healthcare) in the medium and by NK cytotoxicity against B16D8. Cytotoxicity was determined by standard ^{51}Cr release assay as described previously (Akazawa et al., 2007a).

Ex vivo NK activation. Mice were i.p. injected with 250 μg polyI:C. After 24 h, spleen cells were harvested and then NK cells ($DX5^+$ cells) were positively isolated with the MACS system (Miltenyi Biotec). The $DX5^+$ NK cells were suspended in RPMI1640 with 10% FCS and mixed with ^{51}Cr-labeled B16D8 cells at indicated E/T ratios. After 4 h, supernatants were harvested and ^{51}Cr release was measured. Specific lysis was calculated by (specific release − spontaneous release)/(max release − spontaneous release). In some experiments, blood was drawn from the eyes of mice 8 h after polyI:C administration for cytokine measurement.

Test for in vivo NK activation in LN. 5×10^5 WT BMDCs incubated with or without 10 μg/ml polyI:C for 24 h or 5×10^5 IRF-$3^{-/-}$ BMDCs infected with control virus or INAM-expressing lentivirus and allowed to stand for 24 h were injected into the footpads of WT C57BL/6 mice. 48 h later, cells in their inguinal LN were harvested, stained with PE-DX5, and sorted by FACSAria II. RNA was extracted from the DX5-positive cells with TRIzol.

DC therapy. DC therapy against mice with B16D8 tumor burden was described previously (Akazawa et al., 2007a). C57BL/6 mice ($n = 3$) were shaved at the flank and injected s.c. with 6×10^5 syngeneic B16D8 melanoma cells (indicated as day 0). For DC therapy, BMDCs were prepared by transfecting control lentivirus or INAM-expressing lentivirus (INAM/pLenti-IRES-hrGFP) and cultured for 24 h. At the time point indicated in the figures, 10^6 BMDCs were injected s.c. near the tumor. To deplete NK cells in vivo, mice were i.p. injected with hybridoma ascites of anti-NK1.1 mAb (PK136; Akazawa et al., 2007a). Tumor volumes were measured using a caliper every 1 or 2 d. Tumor volume was calculated using the formula: tumor volume (cm^3) = (long diameter) × (short diameter) × (short diameter) × 0.4.

Statistical analysis. Statistical analyses were made with the Student's *t* test. The p-value of significant differences is reported.

Online supplemental material. TICAM-1–inducible genes encoding putative membrane proteins relevant for this study are summarized in Table S1. Fig. S1 shows KO mice results suggesting that both IPS-1 and TICAM-1 in BMDC participate in polyI:C-driven NK activation. Data presented in Fig. S2 characterizes the in vivo polyI:C response of INAM in LN cells. Figs. S3 and S4 demonstrate the properties of surface-expressed INAM analyzed by immunoprecipitation/blotting and confocal microscopy, respectively. Fig. S5 mentions the cytokine expression and maturation profiles of INAM-overexpressing BMDC. Fig. S6 shows the effect of gene silencing of INAM on the polyI:C-mediated cytokine-inducing profile in BMDC. Two pieces of data presented in Fig. S7 confirm the presence of the INAM protein in INAM lentivirus-transduced BMDCs and NK cells. Online supplemental material is available at http://www.jem.org/cgi/content/full/jem.20091573/DC1.

We thank Drs. T. Akazawa and N. Inoue (Osaka Medical Center for Cancer, Osaka, Japan) for their valuable discussions. Thanks are also due to many discussions by our laboratory members. Particularly, extensive English review by Dr. Hussein H. Aly is gratefully acknowledged.

This project was supported by Grants-in-Aid from the Ministry of Education, Science, and Culture and the Ministry of Health, Labor, and Welfare of Japan, Mitsubishi Foundation, Mochida Foundation, NorthTec Foundation Waxman Foundation, and Yakult Foundation.

The authors declare no financial or commercial conflict of interest.

Submitted: 20 July 2009
Accepted: 13 October 2010

REFERENCES

Akazawa, T., T. Ebihara, M. Okuno, Y. Okuda, M. Shingai, K. Tsujimura, T. Takahashi, M. Ikawa, M. Okabe, N. Inoue, et al. 2007a. Antitumor NK activation induced by the Toll-like receptor 3-TICAM-1 (TRIF) pathway in myeloid dendritic cells. *Proc. Natl. Acad. Sci. USA.* 104:252–257. doi:10.1073/pnas.0605978104

Akazawa, T., M. Shingai, M. Sasai, T. Ebihara, N. Inoue, M. Matsumoto, and T. Seya. 2007b. Tumor immunotherapy using bone marrow-derived dendritic cells overexpressing Toll-like receptor adaptors. *FEBS Lett.* 581:3334–3340. doi:10.1016/j.febslet.2007.06.019

Azuma, M., R. Sawahata, Y. Akao, T. Ebihara, S. Yamazaki, M. Matsumoto, M. Hashimoto, K. Fukase, Y. Fujimoto, and T. Seya. 2010. The peptide sequence of diacyl lipopeptides determines dendritic cell TLR2-mediated NK activation. *PLoS One.* 5:e12550. doi:10.1371/journal.pone.0012550

Bertram, L., B.M. Schjeide, B. Hooli, K. Mullin, M. Hiltunen, H. Soininen, M. Ingelsson, L. Lannfelt, D. Blacker, and R.E. Tanzi. 2008. No association between CALHM1 and Alzheimer's disease risk. *Cell.* 135:993–994, author reply :994–996. doi:10.1016/j.cell.2008.11.030

Brandt, C.S., M. Baratin, E.C. Yi, J. Kennedy, Z. Gao, B. Fox, B. Haldeman, C.D. Ostrander, T. Kaifu, C. Chabannon, et al. 2009. The B7 family member B7-H6 is a tumor cell ligand for the activating natural killer cell receptor NKp30 in humans. *J. Exp. Med.* 206:1495–1503. doi:10.1084/jem.20090681

Brilot, F., T. Strowig, S.M. Roberts, F. Arrey, and C. Münz. 2007. NK cell survival mediated through the regulatory synapse with human DCs requires IL-15Ralpha. *J. Clin. Invest.* 117:3316–3329. doi:10.1172/JCI31751

Cerwenka, A., and L.L. Lanier. 2001. Natural killer cells, viruses and cancer. *Nat. Rev. Immunol.* 1:41–49. doi:10.1038/35095564

Cerwenka, A., A.B. Bakker, T. McClanahan, J. Wagner, J. Wu, J.H. Phillips, and L.L. Lanier. 2000. Retinoic acid early inducible genes define a ligand family for the activating NKG2D receptor in mice. *Immunity.* 12:721–727. doi:10.1016/S1074-7613(00)80222-8

Cerwenka, A., J.L. Baron, and L.L. Lanier. 2001. Ectopic expression of retinoic acid early inducible-1 gene (RAE-1) permits natural killer cell-mediated rejection of a MHC class I-bearing tumor in vivo. *Proc. Natl. Acad. Sci. USA.* 98:11521–11526. doi:10.1073/pnas.201238598

Dreses-Werringloer, U., J.C. Lambert, V. Vingtdeux, H. Zhao, H. Vais, A. Siebert, A. Jain, J. Koppel, A. Rovelet-Lecrux, D. Hannequin, et al. 2008. A polymorphism in CALHM1 influences Ca2+ homeostasis,

Downloaded from jem.rupress.org on November 24, 2010

Abeta levels, and Alzheimer's disease risk. *Cell.* 133:1149–1161. doi:10.1016/j.cell.2008.05.048

Ebihara, T., H. Masuda, T. Akazawa, M. Shingai, H. Kikuta, T. Ariga, M. Matsumoto, and T. Seya. 2007. Induction of NKG2D ligands on human dendritic cells by TLR ligand stimulation and RNA virus infection. *Int. Immunol.* 19:1145–1155. doi:10.1093/intimm/dxm073

Fernandez, N.C., A. Lozier, C. Flament, P. Ricciardi-Castagnoli, D. Bellet, M. Suter, M. Perricaudet, T. Tursz, E. Maraskovsky, and L. Zitvogel. 1999. Dendritic cells directly trigger NK cell functions: cross-talk relevant in innate anti-tumor immune responses in vivo. *Nat. Med.* 5:405–411. doi:10.1038/7403

Fitzgerald, K.A., S.M. McWhirter, K.L. Faia, D.C. Rowe, E. Latz, D.T. Golenbock, A.J. Coyle, S.M. Liao, and T. Maniatis. 2003. IKKepsilon and TBK1 are essential components of the IRF3 signaling pathway. *Nat. Immunol.* 4:491–496. doi:10.1038/ni921

Gerosa, F., B. Baldani-Guerra, C. Nisii, V. Marchesini, G. Carra, and G. Trinchieri. 2002. Reciprocal activating interaction between natural killer cells and dendritic cells. *J. Exp. Med.* 195:327–333. doi:10.1084/jem.20010938

Hamerman, J.A., K. Ogasawara, and L.L. Lanier. 2004. Cutting edge: Toll-like receptor signaling in macrophages induces ligands for the NKG2D receptor. *J. Immunol.* 172:2001–2005.

Honda, K., H. Yanai, H. Negishi, M. Asagiri, M. Sato, T. Mizutani, N. Shimada, Y. Ohba, A. Takaoka, N. Yoshida, and T. Taniguchi. 2005. IRF-7 is the master regulator of type-I interferon-dependent immune responses. *Nature.* 434:772–777. doi:10.1038/nature03464

Hornung, V., S. Rothenfusser, S. Britsch, A. Krug, B. Jahrsdörfer, T. Giese, S. Endres, and G. Hartmann. 2002. Quantitative expression of toll-like receptor 1-10 mRNA in cellular subsets of human peripheral blood mononuclear cells and sensitivity to CpG oligodeoxynucleotides. *J. Immunol.* 168:4531–4537.

Huntington, N.D., N. Legrand, N.L. Alves, B. Jaron, K. Weijer, A. Plet, E. Corcuff, E. Mortier, Y. Jacques, H. Spits, and J.P. Di Santo. 2009. IL-15 trans-presentation promotes human NK cell development and differentiation in vivo. *J. Exp. Med.* 206:25–34. doi:10.1084/jem.20082013

Iwasaki, A., and R. Medzhitov. 2004. Toll-like receptor control of the adaptive immune responses. *Nat. Immunol.* 5:987–995. doi:10.1038/ni1112

Kalinski, P., R.B. Mailliard, A. Giermasz, H.J. Zeh, P. Basse, D.L. Bartlett, J.M. Kirkwood, M.T. Lotze, and R.B. Herberman. 2005. Natural killer-dendritic cell cross-talk in cancer immunotherapy. *Expert Opin. Biol. Ther.* 5:1303–1315. doi:10.1517/14712598.5.10.1303

Kato, H., O. Takeuchi, S. Sato, M. Yoneyama, M. Yamamoto, K. Matsui, S. Uematsu, A. Jung, T. Kawai, K.J. Ishii, et al. 2006. Differential roles of MDA5 and RIG-I helicases in the recognition of RNA viruses. *Nature.* 441:101–105. doi:10.1038/nature04734

Kawai, T., K. Takahashi, S. Sato, C. Coban, H. Kumar, H. Kato, K.J. Ishii, O. Takeuchi, and S. Akira. 2005. IPS-1, an adaptor triggering RIG-I- and Mda5-mediated type I interferon induction. *Nat. Immunol.* 6:981–988. doi:10.1038/ni1243

Kubin, M.Z., D.L. Parshley, W. Din, J.Y. Waugh, T. Davis-Smith, C.A. Smith, B.M. Macduff, R.J. Armitage, W. Chin, L. Cassiano, et al. 1999. Molecular cloning and biological characterization of NK cell activation-inducing ligand, a counterstructure for CD48. *Eur. J. Immunol.* 29:3466–3477. doi:10.1002/(SICI)1521-4141(199911)29:11<3466::AID-IMMU3466>3.0.CO;2-9

Lee, A.E., L.A. Rogers, J.M. Longcroft, and R.E. Jeffery. 1990. Reduction of metastasis in a murine mammary tumour model by heparin and polyinosinic-polycytidylic acid. *Clin. Exp. Metastasis.* 8:165–171. doi:10.1007/BF00117789

Levy, S., and T. Shoham. 2005. The tetraspanin web modulates immune-signalling complexes. *Nat. Rev. Immunol.* 5:136–148. doi:10.1038/nri1548

Lucas, M., W. Schachterle, K. Oberle, P. Aichele, and A. Diefenbach. 2007. Dendritic cells prime natural killer cells by trans-presenting interleukin 15. *Immunity.* 26:503–517. doi:10.1016/j.immuni.2007.03.006

Masuda, H., Y. Saeki, M. Nomura, K. Shida, M. Matsumoto, M. Ui, L.L. Lanier, and T. Seya. 2002. High levels of RAE-1 isoforms on mouse tumor cell lines assessed by anti-"pan" RAE-1 antibody confer tumor susceptibility to NK cells. *Biochem. Biophys. Res. Commun.* 290:140–145. doi:10.1006/bbrc.2001.6165

Matsumoto, M., and T. Seya. 2008. TLR3: interferon induction by double-stranded RNA including poly(I:C). *Adv. Drug Deliv. Rev.* 60:805–812. doi:10.1016/j.addr.2007.11.005

McCartney, S., W. Vermi, S. Gilfillan, M. Cella, T.L. Murphy, R.D. Schreiber, K.M. Murphy, and M. Colonna. 2009. Distinct and complementary functions of MDA5 and TLR3 in poly(I:C)-mediated activation of mouse NK cells. *J. Exp. Med.* 206:2967–2976. doi:10.1084/jem.20091181

Medzhitov, R., and C.A. Janeway Jr. 1997. Innate immunity: the virtues of a nonclonal system of recognition. *Cell.* 91:295–298. doi:10.1016/S0092-8674(00)80412-2

Meylan, E., J. Curran, K. Hofmann, D. Moradpour, M. Binder, R. Bartenschlager, and J. Tschopp. 2005. Cardif is an adaptor protein in the RIG-I antiviral pathway and is targeted by hepatitis C virus. *Nature.* 437:1167–1172. doi:10.1038/nature04193

Miyake, T., Y. Kumagai, H. Kato, Z. Guo, K. Matsushita, T. Satoh, T. Kawagoe, H. Kumar, M.H. Jang, T. Kawai, et al. 2009. Poly I:C-induced activation of NK cells by CD8 alpha+ dendritic cells via the IPS-1 and TRIF-dependent pathways. *J. Immunol.* 183:2522–2528. doi:10.4049/jimmunol.0901500

Mukai, M., F. Imamura, M. Ayaki, K. Shinkai, T. Iwasaki, K. Murakami-Murofushi, H. Murofushi, S. Kobayashi, T. Yamamoto, H. Nakamura, and H. Akedo. 1999. Inhibition of tumor invasion and metastasis by a novel lysophosphatidic acid (cyclic LPA). *Int. J. Cancer.* 81:918–922. doi:10.1002/(SICI)1097-0215(19990611)81:6<918::AID-IJC13>3.0.CO;2-E

Newman, K.C., and E.M. Riley. 2007. Whatever turns you on: accessory-cell-dependent activation of NK cells by pathogens. *Nat. Rev. Immunol.* 7:279–291. doi:10.1038/nri2057

Nomura, M., Z. Zou, T. Joh, Y. Takihara, Y. Matsuda, and K. Shimada. 1996. Genomic structures and characterization of Rae1 family members encoding GPI-anchored cell surface proteins and expressed predominantly in embryonic mouse brain. *J. Biochem.* 120:987–995.

Ohteki, T., H. Tada, K. Ishida, T. Sato, C. Maki, T. Yamada, J. Hamuro, and S. Koyasu. 2006. Essential roles of DC-derived IL-15 as a mediator of inflammatory responses in vivo. *J. Exp. Med.* 203:2329–2338. doi:10.1084/jem.20061297

Oshiumi, H., M. Matsumoto, K. Funami, T. Akazawa, and T. Seya. 2003a. TICAM-1, an adaptor molecule that participates in Toll-like receptor 3-mediated interferon-beta induction. *Nat. Immunol.* 4:161–167. doi:10.1038/ni886

Oshiumi, H., M. Sasai, K. Shida, T. Fujita, M. Matsumoto, and T. Seya. 2003b. TIR-containing adapter molecule (TICAM)-2, a bridging adapter recruiting to toll-like receptor 4 TICAM-1 that induces interferon-beta. *J. Biol. Chem.* 278:49751–49762. doi:10.1074/jbc.M305820200

Sasai, M., M. Shingai, K. Funami, M. Yoneyama, T. Fujita, M. Matsumoto, and T. Seya. 2006. NAK-associated protein 1 participates in both the TLR3 and the cytoplasmic pathways in type I IFN induction. *J. Immunol.* 177:8676–8683.

Sato, M., H. Suemori, N. Hata, M. Asagiri, K. Ogasawara, K. Nakao, T. Nakaya, M. Katsuki, S. Noguchi, N. Tanaka, and T. Taniguchi. 2000. Distinct and essential roles of transcription factors IRF-3 and IRF-7 in response to viruses for IFN-alpha/beta gene induction. *Immunity.* 13:539–548. doi:10.1016/S1074-7613(00)00053-4

Seth, R.B., L. Sun, C.K. Ea, and Z.J. Chen. 2005. Identification and characterization of MAVS, a mitochondrial antiviral signaling protein that activates NF-kappaB and IRF 3. *Cell.* 122:669–682. doi:10.1016/j.cell.2005.08.012

Seya, T., and M. Matsumoto. 2009. The extrinsic RNA-sensing pathway for adjuvant immunotherapy of cancer. *Cancer Immunol. Immunother.* 58:1175–1184. doi:10.1007/s00262-008-0652-9

Sivori, S., M. Falco, M. Della Chiesa, S. Carlomagno, M. Vitale, L. Moretta, and A. Moretta. 2004. CpG and double-stranded RNA trigger human NK cells by Toll-like receptors: induction of cytokine release and cytotoxicity against tumors and dendritic cells. *Proc. Natl. Acad. Sci. USA.* 101:10116–10121. doi:10.1073/pnas.0403744101

Tanaka, H., Y. Mori, H. Ishii, and H. Akedo. 1988. Enhancement of metastatic capacity of fibroblast-tumor cell interaction in mice. *Cancer Res.* 48:1456–1459.

Downloaded from jem.rupress.org on November 24, 2010

Tsuji, S., J. Uehori, M. Matsumoto, Y. Suzuki, A. Matsuhisa, K. Toyoshima, and T. Seya. 2001. Human intelectin is a novel soluble lectin that recognizes galactofuranose in carbohydrate chains of bacterial cell wall. *J. Biol. Chem.* 276:23456–23463. doi:10.1074/jbc.M103162200

Vivier, E., E. Tomasello, M. Baratin, T. Walzer, and S. Ugolini. 2008. Functions of natural killer cells. *Nat. Immunol.* 9:503–510. doi:10.1038/ni1582

Xu, L.G., Y.Y. Wang, K.J. Han, L.Y. Li, Z. Zhai, and H.B. Shu. 2005. VISA is an adapter protein required for virus-triggered IFN-beta signaling. *Mol. Cell.* 19:727–740. doi:10.1016/j.molcel.2005.08.014

Yamamoto, M., S. Sato, H. Hemmi, K. Hoshino, T. Kaisho, H. Sanjo, O. Takeuchi, M. Sugiyama, M. Okabe, K. Takeda, and S. Akira. 2003a. Role of adaptor TRIF in the MyD88-independent toll-like receptor signaling pathway. *Science.* 301:640–643. doi:10.1126/science.1087262

Yamamoto, M., S. Sato, H. Hemmi, S. Uematsu, K. Hoshino, T. Kaisho, O. Takeuchi, K. Takeda, and S. Akira. 2003b. TRAM is specifically involved in the Toll-like receptor 4-mediated MyD88-independent signaling pathway. *Nat. Immunol.* 4:1144–1150. doi:10.1038/ni986

Yoneyama, M., M. Kikuchi, T. Natsukawa, N. Shinobu, T. Imaizumi, M. Miyagishi, K. Taira, S. Akira, and T. Fujita. 2004. The RNA helicase RIG-I has an essential function in double-stranded RNA-induced innate antiviral responses. *Nat. Immunol.* 5:730–737. doi:10.1038/ni1087

Zanoni, I., M. Foti, P. Ricciardi-Castagnoli, and F. Granucci. 2005. TLR-dependent activation stimuli associated with Th1 responses confer NK cell stimulatory capacity to mouse dendritic cells. *J. Immunol.* 175:286–292.

Zou, Z., M. Nomura, Y. Takihara, T. Yasunaga, and K. Shimada. 1996. Isolation and characterization of retinoic acid-inducible cDNA clones in F9 cells: a novel cDNA family encodes cell surface proteins sharing partial homology with MHC class I molecules. *J. Biochem.* 119:319–328.

Downloaded from jem.rupress.org on November 24, 2010

Published November 8, 2010

JEM

SUPPLEMENTAL MATERIAL

Ebihara et al., http://www.jem.org/cgi/content/full/jem.20091573/DC1

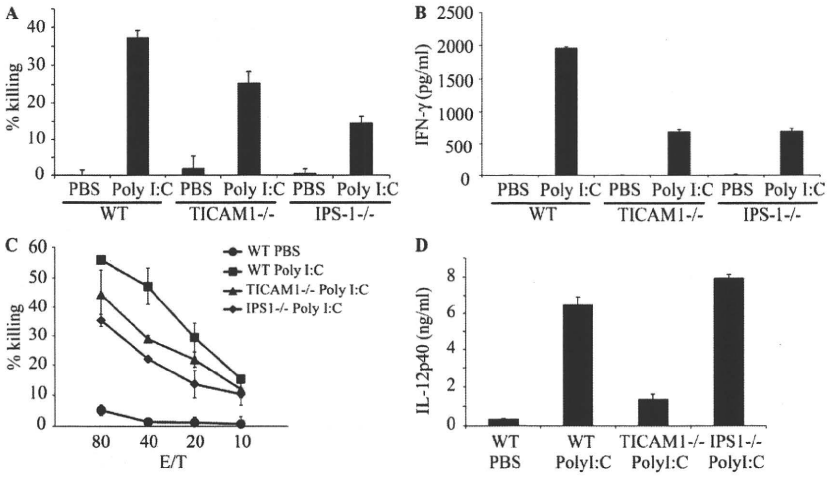

Figure S1. KO mice results suggest that both IPS-1 and TICAM-1 in BMDC participate in polyI:C-driven NK activation. (A and B) IPS-1 and TICAM-1 in BMDC participate in polyI:C-driven NK activation. 2.5 × 10^5 BMDCs prepared from WT, TICAM1$^{-/-}$, and IPS1$^{-/-}$ mice were incubated with 5 × 10^5 NK cells in the presence or absence (PBS) of 50 µg/ml polyI:C for 24 h. Then, the supernatants were harvested for IFN-γ ELISA (B). To determine NK cytotoxicity, ^{51}Cr-labeled B16D8 cells were added to the culture and, 4 h later, released ^{51}Cr was measured (A). One representative of three similar experiments is shown. (C) Both IPS-1 and TICAM-1 participate in in vivo polyI:C-induced NK activation. WT, IPS-1$^{-/-}$, and TICAM-1$^{-/-}$ mice were i.p. injected with 250 µg polyI:C. After 24 h, NK cells were harvested by DX5-MACS beads from spleen and used as effector cells in a cytotoxic assay with ^{51}Cr-labeled B16D8 targets. Cytotoxic activity of NK cells was measured under the indicated E/T ratios 4 h after the E/T mixing. One representative of the three similar experiments is shown. (D) Increasing serum level of IL-12p40 is dependent on TICAM-1. 250 µg polyI:C was i.p. injected into a series of mice as in B. 8 h after injection of polyI:C, blood serum was collected to determine the levels of IL-12p40 by ELISA. Although it is not depicted, IL-12p70 was not detected in these samples by ELISA. Data in A–D represent mean ± SD.

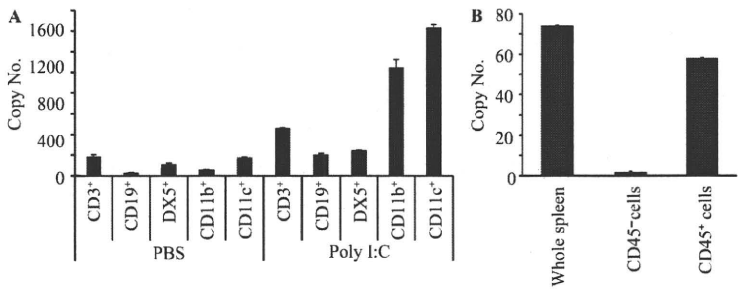

Figure S2. In vivo polyI:C response of INAM in LN cells. (A) Up-regulation of INAM expression in LN cells by polyI:C injection. WT C57BL/6 mice were i.p. injected with 100 µg polyI:C or control buffer. After 24 h, inguinal, axillary, and mesenteric LN were harvested. Cell populations with indicated markers were separated by FACS sorting, and the INAM mRNA level of each population was determined by real-time PCR. (B) CD45$^+$ cells express INAM. Splenocytes were separated into CD45$^-$ and CD45$^+$ cells after the polyI:C injection as in A. The INAM mRNA levels of the two populations were determined by real-time PCR. Representative data from one of three experiments are shown. Data in A and B represent mean ± SD.

Downloaded from jem.rupress.org on November 24, 2010

Published November 8, 2010

JEM

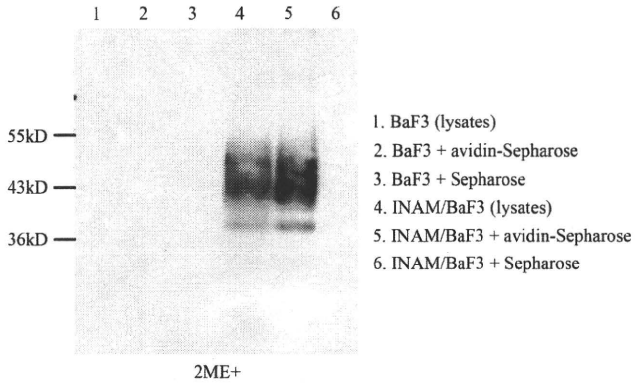

Figure S3. INAM is expressed on cell surface. Membrane proteins of Flag-tagged INAM-expressing BaF3 (INAM/BaF3) and control BaF3 were biotinylated and solubilized. Biotinylated proteins were immunoprecipitated by Avidin-Sepharose or control Sepharose. After electrophoresis on SDS-PAGE, INAM was detected by anti-Flag M2 mAb.

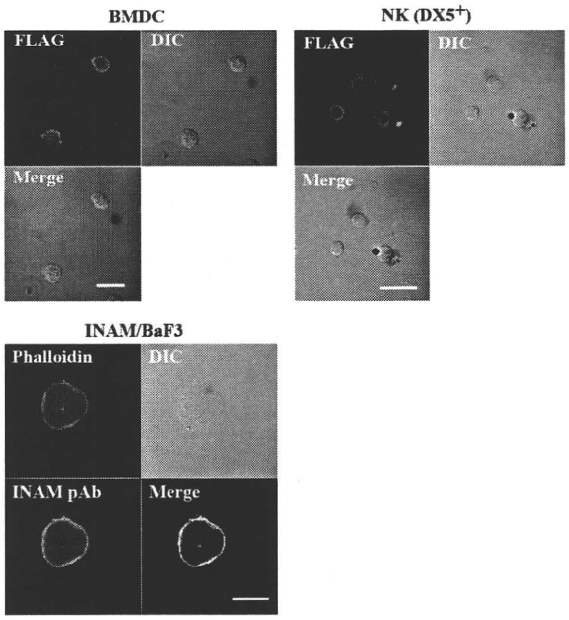

Figure S4. Confocal analysis of surface-expressed INAM. WT BMDC (left) or NK cells (right) were infected with INAM-expressing vector and stained with anti-FLAG mAb (Alexa Fluor 568). Stable Ba/F3 transfectants expressing INAM (bottom) were permeabilized and stained with phalloidin and anti-INAM pAb, followed by Alexa Fluor 488–conjugated secondary antibody. Cells were analyzed on a confocal laser-scanning microscope (LSM 510 META). Bars, 20 μm.

Downloaded from jem.rupress.org on November 24, 2010

Published November 8, 2010

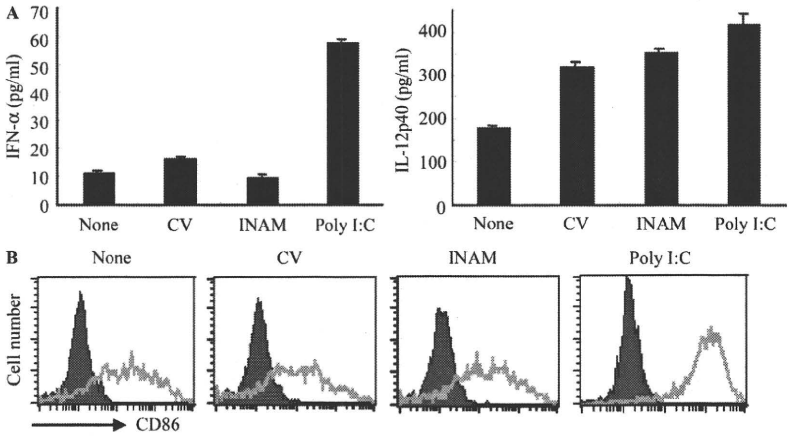

Figure S5. INAM-overexpressing BMDC did not induce cytokine responses and maturation. WT BMDCs were transfected with control lentivirus (CV) or INAM-expressing lentivirus (INAM-virus) and cultured for 24 h. (A) ELISA of IFN-α and IL-12p40 in the culture supernatants. Data shown are means ± SD of triplicate samples from one experiment representative of three. (B) Flow cytometry for CD86 in the transfected BMDC. Polyl:C stimulation (10 μg/ml) was used for positive control.

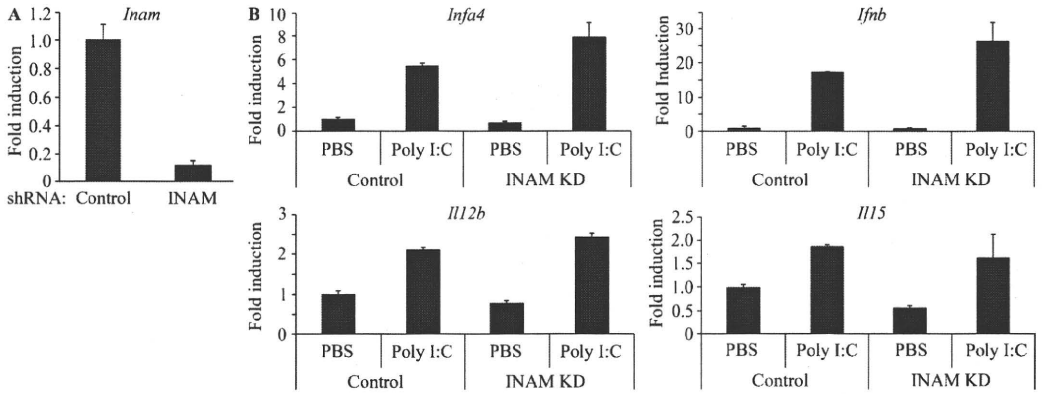

Figure S6. The effect of gene silencing of INAM on the polyI:C-mediated cytokine inducing profile in BMDC. (A) Gene silencing of INAM in BMDC. 5 × 10^5 WT BMDCs were infected with INAM shRNA-generating lentivirus or control lentivirus. After 36 h, the levels of INAM mRNA expression were assessed by real time PCR. Data show one of three similar experiments. (B) Effect of BMDC INAM on cytokine expression. INAM in 5 × 10^5 WT BM-DCs was silenced as in A. Then, control or INAM-silenced BMDC were stimulated with 10 μg/ml polyI:C for 8 h. RNA was harvested from BMDC with RNeasy and the levels of indicated mRNA were determined by real-time PCR. Data show one of two similar experimental results. Data in A and B represent mean ± SD.

Downloaded from jem.rupress.org on November 24, 2010

Published November 8, 2010

JEM

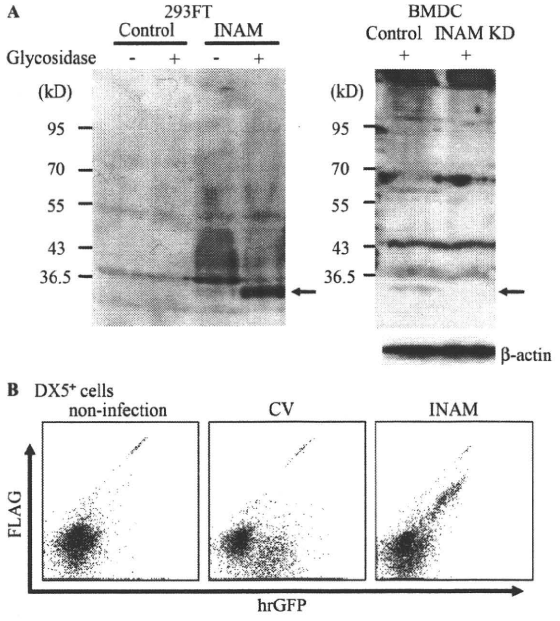

Figure S7. Detection of the INAM protein in DCs and NK cells. (A) Detection of the endogenous INAM protein in BMDC. 5×10^6 BMDCs were transduced with INAM-shRNA or control shRNA-expressing lentivirus. 48 h later, these cells were lysed and treated with *N*-glycosidase F for 2 h at 37°C. All cell lysates were subjected to SDS-PAGE and immunoblotted by rabbit anti-INAM pAb. The cell lysates from 293FT cells transfected with pEFBOS or pEFBOS/INAM were used as negative and positive control, respectively. Arrows indicate the band for INAM. Mr markers are shown to the left. One of three similar experiments is shown. (B) $DX5^+$ NK cells express GFP and FLAG, markers for INAM. 5×10^5 $DX5^+$ cells were transduced with control or INAM-expressing lentivirus for 48 h. Then, these cells were permeabilized and stained with rabbit anti-FLAG pAb and PE-anti rabbit IgG. Levels of FLAG and hrGFP, reflecting INAM expression, were measured by FACSCalibur. Experiments were performed more than six times with different conditions and representative data are shown.

Table S1. TICAM-1-inducible genes encoding putative membrane or GPI-anchored proteins

Official symbol	Other aliases	UniGene ID	Fold induction (poly I:C stimulation/nonstimulation)			
			WT	MyD88$^{-/-}$	TLR3$^{-/-}$	TICAM-1$^{-/-}$
Aplnr	APJ, Agtrl1, msr/apj	Mm.29368	2.074101377	0.79485698	0.24913528	0.296911294
Fam26f	INAM, A630077B13Rik	Mm.34479	15.57360865	8.048081457	0.939239821	1.221297574
Clec4e	Clecsf9, Mincle	Mm.248327	5.65851862	7.142025946	2.761541794	2.087684899
Ly6i	Ly-6M, AI789751	Mm.358339	5.679941154	26.36364231	0.734513568	1.09611157
Slamf8	Blame, SBBI42	Mm.179812	6.814581008	5.127202394	1.802731559	1.122849288
Tmem171	Gm905, MGC117733	Mm.28264	12.42279971	7.454421156	2.274145126	3.051240138
Pvrl4	1200017F15Rik, Prr4	Mm.263414	5.02297837	4.096701442	1.627391239	1.961829994
Vcam1	CD106	Mm.76649	4.742423155	4.572993249	0.948952117	0.554171652
Tnfsf10	APO-2L, TL2, Trail	Mm.1062	41.9745751	30.22262268	6.007858781	2.631939934

Downloaded from jem.rupress.org on November 24, 2010

Hepatology Research

Hepatology Research 2010; **40**: 1248–1253 doi: 10.1111/j.1872-034X.2010.00730.x

Short Communication

Gene expression profile of Li23, a new human hepatoma cell line that enables robust hepatitis C virus replication: Comparison with HuH-7 and other hepatic cell lines

Kyoko Mori,* Masanori Ikeda, Yasuo Ariumi and Nobuyuki Kato*

Department of Tumor Virology, Okayama University Graduate School of Medicine, Dentistry and Pharmaceutical Sciences, Okayama, Japan

Aim: Human hepatoma cell line HuH-7-derived cells are currently the only cell culture system used for robust hepatitis C virus (HCV) replication. We recently found a new human hepatoma cell line, Li23, that enables robust HCV replication. Although both cell lines had similar liver-specific expression profiles, the overall profile of Li23 seemed to differ considerably from that of HuH-7. To understand this difference, the expression profile of Li23 cells was further characterized by a comparison with that of HuH-7 cells.

Methods: cDNA microarray analysis using Li23 and HuH-7 cells was performed. Li23-derived ORL8c cells and HuH-7-derived RSc cells, in which HCV could infect and efficiently replicate, were also used for the microarray analysis. For the comparative analysis by reverse transcription polymerase chain reaction (RT–PCR), human hepatoma cell lines (HuH-6, HepG2, HLE, HLF and PLC/PRF/5) and immortalized hepatocyte cell line (PH5CH8) were also used.

Results: Microarray analysis of Li23 versus HuH-7 cells selected 80 probes to represent highly expressed genes that have ratios of more than 30 (Li23/HuH-7) or 20 (HuH-7/Li23). Among them, 17 known genes were picked up for further analysis. The expression levels of most of these genes in Li23 and HuH-7 cells were retained in ORL8c and RSc cells, respectively. Comparative analysis by RT–PCR using several other hepatic cell lines resulted in the classification of 17 genes into three types, and identified three genes showing Li23-specific expression profiles.

Conclusion: Li23 is a new hepatoma cell line whose expression profile is distinct from those of frequently used hepatic cell lines.

Key words: hepatitis C virus, hepatoma cell line, HuH-7, Li23, microarray

INTRODUCTION

HUH-7, A HUMAN hepatoma cell line,[1] is frequently used in the research of hepatitis C virus (HCV), since an HCV replicon system enabling HCV subgenomic RNA replication was developed using HuH-7 cells.[2] Even with the use of an efficient HCV production system developed in 2005,[3] HuH-7-derived cells are still used as the only cell line for persistent HCV production systems.

We previously developed HCV replicon systems[4,5] and an HCV production system[6] using HuH-7-derived cells. Furthermore, we recently found a new human hepatoma cell line, Li23, that enables robust HCV RNA replication and persistent HCV production.[7] In that study, using microarray analysis, we excluded the possibility that the obtained Li23-derived cells were derived from contamination of HuH-7-derived cells used for HCV replication.[7] In addition, we noticed that the gene expression profile of Li23 cells seemed considerably different from that of HuH-7 cells. Therefore, we assumed that the Li23 cell line possesses a unique expression profile among widely used human hepatoma cell lines. To evaluate this assumption, we further characterized the expression profile of Li23 cells by comparing it with those of other human hepatoma cell lines, including HuH-7,[1] HuH-6,[8] HepG2,[9] HLE,[10] HLF[10] and PLC/PRF/5.[11] Human immortalized hepatocyte cell line

Correspondence: Professor Nobuyuki Kato, Department of Tumor Virology, Okayama University Graduate School of Medicine, Dentistry and Pharmaceutical Sciences, Okayama 700-8558, Japan. Email: nkato@md.okayama-u.ac.jp

*These authors contributed equally to this work.

Received 21 July 2010; revision 16 August 2010; accepted 17 August 2010.

© 2010 The Japan Society of Hepatology

PH5CH8[12] was also used for the comparison. Here, we show that the Li23 cell line possesses a distinct expression profile among hepatic cell lines.

METHODS

Cell culture

HUH-7, HUH-6, HEPG2, HLE, HLF and PLC/PRF/5 cells were cultured in Dulbecco's modified Eagle's medium supplemented with 10% fetal bovine serum. Li23 and PH5CH8 cells were maintained as described previously.[7] Cured cells (Li23-derived ORL8c and HuH-7-derived RSc), from which the HCV RNA had been eliminated by interferon (IFN) treatment, were also maintained as described previously.[7]

cDNA microarray analysis

Li23, ORL8c, HuH-7 and RSc cells (1×10^6 each) were plated onto 10-cm diameter dishes and cultured for 2 days. Total RNA from these cells were prepared using the RNeasy extraction kit (QIAGEN, Hilden, Germany). cDNA microarray analysis was performed according to the methods described previously.[7] Differentially expressed genes were selected by comparing the arrays from Li23 and HuH-7 cells. The selected genes were further compared with the array from ORL8c or RSc cells.

Reverse transcription polymerase chain reaction

Reverse transcription polymerase chain reaction (RT-PCR) was performed to detect cellular mRNA as described previously.[13] Briefly, total RNA (2 μg) was reverse-transcribed with M-MLV reverse transcriptase (Invitrogen, San Diego, CA, USA) using an oligo dT primer (Invitrogen) according to the manufacturer's protocol. One-tenth of the synthesized cDNA was used for PCR. The primers arranged for this study are listed in Table 1. In addition, we used primer sets for New York esophageal squamous cell carcinoma 1 (NY-ESO-1), β-defensin-1 (DEFB1), lectin, galactoside-binding, soluble 3 (LGALS3)/Galectin-3, melanoma-specific antigen family A6 (MAGEA6), UDP glycosyltransferase 2 family polypeptide B4 (UGT2B4), transmembrane 4 superfamily member 3 (TM4SF3), insulin-like growth factor binding protein 2 (IGFBP2), arylacetamide deacetylase (AADAC), albumin and glyceraldehyde-3-phosphate dehydrogenase (GAPDH), as described previously.[7]

RESULTS

Genes showing pronounced differences in gene expression between Li23- and HuH-7-derived cells

WE RECENTLY ESTABLISHED several Li23-derived cell lines showing robust HCV RNA replication.[7] In convenient microarray analysis using these cell lines, we noticed that the gene expression profile of Li23 cells differed considerably from that of HuH-7 cells, and that several genes, including cancer antigens such as NY-ESO-1 and MAGEA6, were highly expressed in Li23 cells but were not expressed in HuH-7 cells.[7] However, it

Table 1 Primers used for reverse transcription polymerase chain reaction analysis

Gene (accession no.)	Direction	Nucleotide sequence (5′–3′)	Products (bp)
Cancer antigen 45, A5	Forward	TGGAGATGACCTAGAATGCAG	218
(CT45A5); NM_001007551	Reverse	CTCGTCTCATACATCTTGCTG	
Four-and-a-half LIM domain 1	Forward	GGAATCACTTACCAGGATCAG	243
(FHL1; NM_001449)	Reverse	TTTGCAGTGGAAGCAGTAGTC	
Thymosin β4, X-linked	Forward	ACCAGACTTCGCTCGTACTC	179
(TMSB4X; NM_021109)	Reverse	TCGCCTGCTTGCTTCTCCTG	
Lectin, galactoside-binding, soluble 1	Forward	CAACACCATCGTGTGCAACAG	253
(LGALS1; NM_002305)	Reverse	CAGCTGCCATGTAGTTGATGG	
Interferon-induced transmembrane protein 2	Forward	CCTCTTCATGAACACCTGCTG	184
(IFITM2; NM_006435)	Reverse	CACTGGGATGATGATGAGCAG	
Apolipoproteins A1	Forward	ACTGTGTACGTGGATGTGCTC	273
(APOA1; X02162)	Reverse	CTTCTTCTGGAAGTCGTCCAG	
α-2-HS-glycoprotein	Forward	AACCGAACTGCGATGATCCAG	248
(AHSG; NM_001622)	Reverse	TTCGACAGCATGCTCCTTCAG	
Gap junction protein-α 1	Forward	CATCTTCATGCTGGTGGTGTC	253
(GJA1; NM_000165)	Reverse	GTTTCTGTCGCCAGTAACCAG	

© 2010 The Japan Society of Hepatology

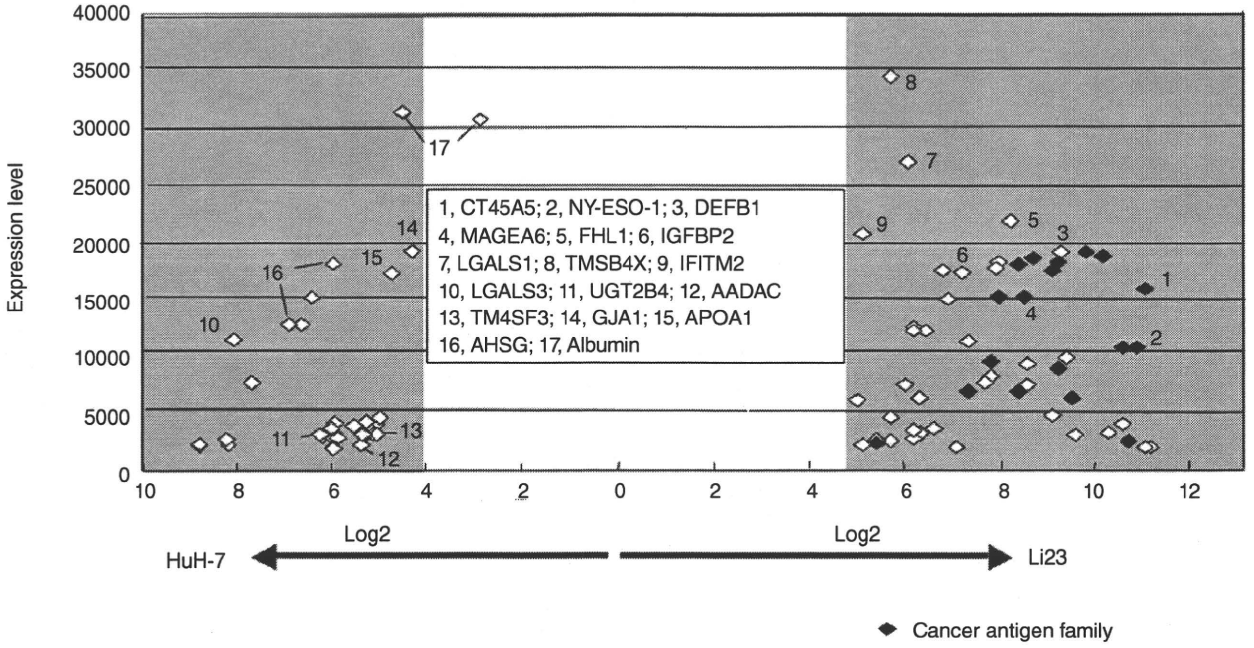

Figure 1 Genes showing pronounced differences in gene expression between Li23 and HuH-7 cells. The probes showing expression levels of more than 2000 and ratios of more than 30 (Li23/HuH-7) or 20 (HuH-7/Li23) are presented.

is unclear whether the expression profiles of these genes are characteristics of Li23 cells.

To clarify this point, comprehensive microarray analysis using Li23 and HuH-7 cells was performed. This revealed 4119 and 3570 probes whose expression levels were upregulated and downregulated at ratios of more than 2 and less than 0.5 in Li23 versus HuH-7 cells, respectively. From among these probes, we selected those showing ratios of more than 30 (Li23/HuH-7) and 20 (HuH-7/Li23), and further selected the probes showing expression levels of more than 2000 (actual value of measurement). By these selections, 80 probes were assigned (Fig. 1). The most distinguishing characteristic of the comparison is that the cancer antigen family (18 probes) was highly expressed in Li23 cells but was not highly expressed in HuH-7 cells (Fig. 1). From these probes, 14 known genes showing expression levels above 10 000 (#1–10 and #14–17 in Fig. 1) and three additional known genes (#11–13 in Fig. 1) were chosen as representative genes for further analysis.

Regarding the total of 17 genes, the expression levels in Li23 versus ORL8c or HuH-7 versus RSc were compared. The expression levels of most of the 17 genes were maintained between Li23 and ORL8c cells or between HuH-7 and RSc cells (Table 2). These results indicate that ORL8c and RSc cells retained the characteristics of parent Li23 and HuH-7 cells, respectively. However, it was notable that the expression levels of apolipoprotein A1 (APOA1), α-2-HS-glycoprotein (AHSG), and albumin were significantly higher in ORL8c cells than in Li23 cells, suggesting that ORL8c is selected as a specific clone from Li23 cell populations.

Expression profiles of representative genes whose expression levels showed drastic differences between Li23 and HuH-7 cells among human hepatic cell lines

Regarding the 17 genes selected above, we performed comparative analyses by RT–PCR using Li23, HuH-7, HuH-6, HepG2, HLE, HLF, PLC/PRF/5 and PH5CH8 cells in order to clarify whether or not these genes exhibit Li23-specific expression profiles. The results of the RT–PCR performed after optimization of PCR conditions in each gene resulted in the classification of the 17 genes into three types (A, B and C in Fig. 2). NY-ESO-1 and DEFB1 (high expression in Li23 only), and LGALS3/Galectin-3 (no expression in Li23 only) belonged to type A, which showed a Li23-specific feature. Type B showed that the expression levels in Li23, HLE, HLF, PLC/PRF/5 and/or PH5CH8 cells were greatly higher or lower than those in HuH-7, HuH-6 and HepG2 cells. Type B consisted of cancer antigen 45, A5

© 2010 The Japan Society of Hepatology

Table 2 Representative genes showing pronounced differences in gene expression between Li23 and HuH-7 cells

Gene	Accession no.	Li23	Li23-derived ORL8c	HuH-7	HuH-7-derived RSc
Cancer antigen 45, A5 (CT45A5)	NM_001007551	15 857†	10 508	8	23
Cancer testis antigen 1A (NY-ESO-1/CTAG1A)	U87459	9 005	5 503	5	8
β-Defensin-1 (DEFB1)	U73945	18 311	8 326	31	7
Melanoma-specific antigen family A6 (MAGEA6)	U10691	15 168	17 050	42	35
Four-and-a-half LIM domain 1 (FHL1)	NM_001449	21 851	13 428	77	79
Insulin-like growth factor binding protein 2 (IGFBP2)	NM_000597	17 429	8 931	117	13
Lectin, galactoside-binding, soluble 1 (LGALS1)	NM_002305	26 694	27 098	379	11
Thymosin β4, X-linked (TMSB4X)	NM_021109	34 273	26 199	648	307
IFN-induced transmembrane protein 2 (IFITM2)	NM_006435	20 762	9 645	595	637
Lectin, galactoside-binding, soluble 3 (LGALS3/Galectin 3)	BC001120	41	70	10 973	6 020
UDP glycosyltransferase 2 family polypeptide B4 (UGT2B4)	NM_021139	40	57	2 863	7 546
Arylacetamide deacetylase (AADAC)	NM_001086	57	73	2 282	4 746
Transmembrane 4 superfamily member 3 (TM4SF3)	NM_004616	95	51	3 220	1 265
Gap junction protein-α 43 KDa (GJA1)	NM_000165	951	2	19 090	19 485
Apolipoprotein A1 (APOA1)	X02162	673	7 230	16 920	15 202
α-2-HS-glycoprotein (AHSG)	NM_001622	308	6 373	18 436	26 000
Albumin	AF116645	4 304	30 111	30 234	33 140
	D16931	1 387	23 615	30 668	39 144

†Signal intensity in human genome U133 Plus 2.0 array.

(CT45A5), MAGEA6, four-and-a-half LIM domains 1 (FHL1), Thymosin B4, X-linked (TMSB4X), lectin, galactoside-binding, soluble 1 (LGALS1) and IFN-induced transmembrane protein 2 (IFITM2) – all of which were highly expressed in Li23 cells – and APOA1, AHSG and UGT2B4, which were highly expressed in HuH-7 cells. The remaining five genes were assigned to type C and showed more complex expression profiles (Fig. 2). For instance, Gap junction protein-α 43 kDa (GJA1) expression was observed in HuH-7, HLE, HLF, PLC/PRF/5 and PH5CH8 cell lines, but not in Li23, HuH-6 or HepG2 cell lines. In addition, IGFBP2 expression was observed in Li23, HuH-6 and PH5CH8 cell lines, but not in the other cell lines. Together, these results indicate that the Li23 cell line possesses a distinct expression profile among frequently used hepatic cell lines.

DISCUSSION

IN THIS STUDY, we assigned 17 known genes that showed drastic differences between Li23 and HuH-7 cells, and classified the expression profiles of these genes into at least three types among frequently used hepatic cell lines. Three genes (NY-ESO-1, DEFB1 and LGALS3/Galectin-3) were identified as the representative showing Li23-specific expression.

NY-ESO-1 is a well-characterized cancer-testis antigen (CTAG) that appears to be the most immunogenic CTAG known to date.[14] NY-ESO-1 is expressed in malignant tumors such as melanoma, lung carcinoma and bladder cancer, which are called "CTAG-rich" tumor types, but are expressed solely in the testis among normal adult tissues.[15] Because a spontaneous immune response to NY-ESO-1 is frequently observed in patients with malignant tumors including hepatocellular carcinoma,[16] cancer vaccine trials based on NY-ESO-1 are currently underway.[15] However, the biological role of NY-ESO-1 in both tumors and testis remains poorly understood. Accordingly, the Li23 cell line may be useful for the study of the biological role of NY-ESO-1.

Human defensins, which are small cationic peptides produced by neutrophils and epithelial cells, form two genetically distinct subfamilies, α-defensin and β-defensin. DEFB1, identified in this study, is one of six members belonging to β-defensins and appears to be involved in the antimicrobial defense of the epithelia of surfaces.[16,17] Although α-defensins consisting of six members are known to be expressed in a variety of tumors, DEFB1 is downregulated in some tumor types in which it could behave as a tumor suppressor protein.[18] Our study revealed that except DEFB1 in Li23 cells, no α- or β-defensin members were expressed in the

© 2010 The Japan Society of Hepatology

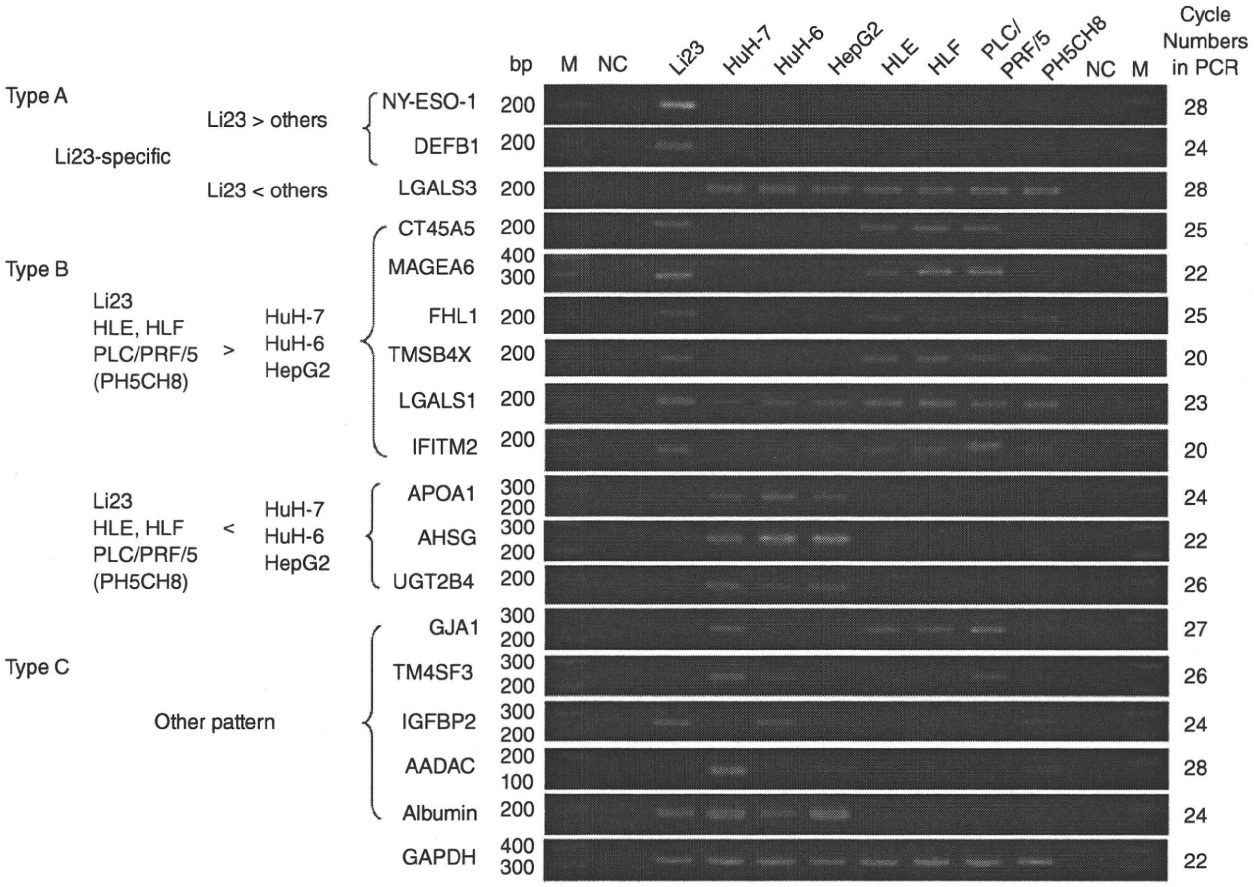

Figure 2 Expression profiles of representative genes, whose expression levels showed drastic differences between Li23 and HuH-7 cells, among human hepatic cell lines. Reverse transcription polymerase chain reaction (RT–PCR) analysis was performed as described in Methods. PCR products were detected by staining with ethidium bromide after separation by electrophoresis on 3% agarose gels.

hepatic cell lines tested in this study (data not shown). Because the molecular mechanism underlying DEFB1 expression or its role in oncogenesis remains to be clarified, Li23 cells may be useful for a study like that.

LGALS3/Galectin-3 is the most studied member of the galectin family, which is characterized by specific binding of β-galactosides through the carbohydrate-recognition domain.[19] LGALS3/Galectin-3 is ubiquitously expressed in numerous cell and tissue types; it is located in both nuclei and cytoplasm, and is secreted through a non-classical pathway. To date, LGALS3/Galectin-3 was found to be involved in many regulations including development, immune reaction, tumorigenesis, and tumor growth and metastasis.[19,20] Indeed, the overexpression of LGALS3/Galectin-3 in cirrhotic and hepatocellular carcinoma has also been reported.[21] In such situations, the absence of LGALS3/Galectin-3 expression in the Li23 cell line is a unique feature among hepatic cell lines, which show high expression levels. Accordingly, the Li23 cell line might be useful as a LGALS3/Galectin-3-null cell line for various studies including those on tumor growth and metastasis.

Although we identified Li23-specific genes showing distinct expression levels among hepatic cell lines examined, microarray analysis revealed that the expression profiles of Li23 and HuH-7 cells, both of which possess an environment for robust HCV replication, differed considerably. Accordingly, such differences may affect the properties or multiplications of HCV, such as susceptibility to anti-HCV reagents, the mutation rate of the HCV genome and the efficiency of HCV replication. Further comparative analysis using Li23 and HuH-7 cells will help to resolve these uncertain subjects.

© 2010 The Japan Society of Hepatology

ACKNOWLEDGMENTS

WE THANK NAOKO Kawahara for her technical assistance. This work was supported by a Grant-in-Aid for research on hepatitis from the Ministry of Health, Labor and Welfare of Japan. K. M. was supported by a Research Fellowship from the Japan Society for Promotion of Science for Young Scientists.

REFERENCES

1 Nakabayashi H, Taketa K, Miyano K, Yamane T, Sato J. Growth of human hepatoma cells lines with differentiated functions in chemically defined medium. *Cancer Res* 1982; **42**: 3858–63.
2 Lohmann V, Körner F, Koch J-O, Herian U, Theilman L, Bartenschlager R. Replication of subgenomic hepatitis C virus RNAs in a hepatoma cell line. *Science* 1999; **285**: 110–13.
3 Wakita T, Pietschmann T, Kato T *et al.* Production of infectious hepatitis C virus in tissue culture from a cloned viral genome. *Nat Med* 2005; **11**: 791–6.
4 Kato N, Sugiyama K, Namba K *et al.* Establishment of a hepatitis C virus subgenomic replicon derived from human hepatocytes infected in vitro. *Biochem Biophys Res Commun* 2003; **306**: 756–66.
5 Ikeda M, Abe K, Dansako H, Nakamura T, Naka K, Kato N. Efficient replication of a full-length hepatitis C virus genome, strain O, in cell culture, and development of a luciferase reporter system. *Biochem Biophys Res Commun* 2005; **329**: 1350–9.
6 Ariumi Y, Kuroki M, Abe K *et al.* DDX3 DEAD-box RNA helicase is required for hepatitis C virus RNA replication. *J Virol* 2007; **81**: 13922–6.
7 Kato N, Mori K, Abe K *et al.* Efficient replication systems for hepatitis C virus using a new human hepatoma cell line. *Virus Res* 2009; **146**: 41–50.
8 Tokiwa T, Doi I, Sato J. Preparation of single cell suspensions from hepatoma cells in culture. *Acta Med Okayama* 1975; **29**: 147–50.
9 Aden DP, Fogel A, Plotkin S, Damjanov I, Knowles BB. Controlled synthesis of HBsAg in a differentiated human liver carcinoma-derived cell line. *Nature* 1979; **282**: 615–16.
10 Doi I, Nambe M, Sato J. Establishment and some biological characteristics of human hepatoma cell lines. *Gann* 1975; **66**: 385–92.
11 Alexander JJ, Bey EM, Geddes EW, Lecatsaa G. Establishment of a continuously growing cell line from primary carcinoma of the liver. *S Afr Med J* 1976; **50**: 2124–8.
12 Ikeda M, Sugiyama K, Mizutani T *et al.* Human hepatocyte clonal cell lines that support persistent replication of hepatitis C virus. *Virus Res* 1998; **56**: 157–67.
13 Dansako H, Naganuma A, Nakamura T, Ikeda F, Nozaki A, Kato N. Differential activation of interferon-inducible genes by hepatitis C virus core protein mediated by the interferon stimulated response element. *Virus Res* 2003; **97**: 17–30.
14 Yoshida N, Abe H, Ohkuri T *et al.* Expression of the MAGE-A4 and NY-ESO-1 cancer-testis antigens and T cell infiltration in non-small cell lung carcinoma and their prognostic significance. *Int J Oncol* 2006; **28**: 1089–98.
15 Caballero OL, Chen YT. Cancer/testis (CT) antigens: potential targets for immunotherapy. *Cancer Sci* 2009; **100**: 2014–21.
16 Korangy F, Ormandy LA, Bleck JS *et al.* Spontaneous tumor-specific humoral and cellular immune responses to NY-ESO-1 in hepatocellular carcinoma. *Clin Cancer Res* 2004; **10**: 4332–41.
17 Bensch KW, Raida M, Magert HJ, Schulz-Knappe P, Forssmann WG. HBD-1: a novel bta-defensin from human plasma. *FEBS Lett* 1995; **368**: 331–5.
18 Droin N, Hendra JB, Ducoroy P, Solary E. Human defensins as cancer biomarkers and antitumour molecules. *J Proteomics* 2009; **72**: 918–27.
19 Dumic J, Dabelic S, Flögel M. Galectin-3: an open-ended story. *Biochim Biophys Acta* 2006; **1760**: 616–35.
20 Danguy A, Camby I, Kiss R. Galectins and cancer. *Biochim Biophys Acta* 2002; **1572**: 285–93.
21 Hsu DK, Dowling CA, Jeng KC, Chen JT, Yang RY, Liu FT. Galectin-3 expression is induced in cirrhotic liver and hepatocellular carcinoma. *Int J Cancer* 1999; **81**: 519–26.

© 2010 The Japan Society of Hepatology

OPEN ACCESS Freely available online

PLoS one

The ESCRT System Is Required for Hepatitis C Virus Production

Yasuo Ariumi[1]*, Misao Kuroki[1], Masatoshi Maki[2], Masanori Ikeda[1], Hiromichi Dansako[1], Takaji Wakita[3], Nobuyuki Kato[1]

1 Department of Tumor Virology, Okayama University Graduate School of Medicine, Dentistry, and Pharmaceutical Sciences, Okayama, Japan, **2** Department of Applied Molecular Biosciences, Graduate School of Bioagricultural Sciences, Nagoya University, Nagoya, Japan, **3** Department of Virology II, National Institute of Infectious Diseases, Tokyo, Japan

Abstract

Background: Recently, lipid droplets have been found to be involved in an important cytoplasmic organelle for hepatitis C virus (HCV) production. However, the mechanisms of HCV assembly, budding, and release remain poorly understood. Retroviruses and some other enveloped viruses require an endosomal sorting complex required for transport (ESCRT) components and their associated proteins for their budding process.

Methodology/Principal Findings: To determine whether or not the ESCRT system is needed for HCV production, we examined the infectivity of HCV or the Core levels in culture supernatants as well as HCV RNA levels in HuH-7-derived RSc cells, in which HCV-JFH1 can infect and efficiently replicate, expressing short hairpin RNA or siRNA targeted to tumor susceptibility gene 101 (TSG101), apoptosis-linked gene 2 interacting protein X (Alix), Vps4B, charged multivesicular body protein 4b (CHMP4b), or Brox, all of which are components of the ESCRT system. We found that the infectivity of HCV in the supernatants was significantly suppressed in these knockdown cells. Consequently, the release of the HCV Core into the culture supernatants was significantly suppressed in these knockdown cells after HCV-JFH1 infection, while the intracellular infectivity and the RNA replication of HCV-JFH1 were not significantly affected. Furthermore, the HCV Core mostly colocalized with CHMP4b, a component of ESCRT-III. In this context, HCV Core could bind to CHMP4b. Nevertheless, we failed to find the conserved viral late domain motif, which is required for interaction with the ESCRT component, in the HCV-JFH1 Core, suggesting that HCV Core has a novel motif required for HCV production.

Conclusions/Significance: These results suggest that the ESCRT system is required for infectious HCV production.

Citation: Ariumi Y, Kuroki M, Maki M, Ikeda M, Dansako H, et al. (2011) The ESCRT System Is Required for Hepatitis C Virus Production. PLoS ONE 6(1): e14517. doi:10.1371/journal.pone.0014517

Editor: Gian Maria Fimia, INMI, Italy

Received May 6, 2010; **Accepted** December 15, 2010; **Published** January 11, 2011

Copyright: © 2011 Ariumi et al. This is an open-access article distributed under the terms of the Creative Commons Attribution License, which permits unrestricted use, distribution, and reproduction in any medium, provided the original author and source are credited.

Funding: This work was supported by a Grant-in-Aid for Scientific Research (C) from the Japan Society for the Promotion of Science (JSPS), by a Grant-in-Aid for Research on Hepatitis from the Ministry of Health, Labor, and Welfare of Japan, by the Viral Hepatitis Research Foundation of Japan, by the Kawasaki Foundation for Medical Science, Medical Welfare, by the Okayama Medical Foundation, and by Ryobi Teien Memory Foundation. MK was supported by a Research Fellowship from the JSPS for Young Scientists. The funders had no role in study design, data collection and analysis, decision to publish, or preparation of the manuscript.

Competing Interests: The authors have declared that no competing interests exist.

* E-mail: ariumi@md.okayama-u.ac.jp

Introduction

Hepatitis C virus (HCV) is a causative agent of chronic hepatitis, which progresses to liver cirrhosis and hepatocellular carcinoma. HCV is an enveloped virus with a positive single stranded 9.6 kb RNA genome, which encodes a large polyprotein precursor of approximately 3,000 amino acid residues. This polyprotein is cleaved by a combination of the host and viral proteases into at least 10 proteins in the following order: Core, envelope 1 (E1), E2, p7, nonstructural protein 2 (NS2), NS3, NS4A, NS4B, NS5A, and NS5B [1]. HCV Core, a highly basic RNA-binding protein, forms a viral capsid and is targeted to lipid droplets [2–6]. The Core is essential for infectious virion production [7]. NS5A, a membrane-associated RNA-binding phosphoprotein, is also involved in the assembly and maturation of infectious HCV particles [8,9]. Intriguingly, NS5A is a key regulator of virion production through the phosphorylation by casein kinase II [9]. Recently, lipid droplets have been found to be involved in an important cytoplasmic organelle for HCV production [4]. Indeed, NS5A is known to colocalize with the Core on lipid droplets [5], and the interaction between NS5A and the Core is critical for the production of infectious HCV particles [3]. However, the host factor involved in HCV assembly, budding, and release remains poorly understood.

Budding is an essential step in the life cycle of enveloped viruses. Endosomal sorting complex required for transport (ESCRT) components and associated factors, such as tumor susceptibility gene 101 (TSG101, a component of ESCRT-I), charged multivesicular body protein 4b (CHMP4b, a component of ESCRT-III), and apoptosis-linked gene 2 interacting protein X (ALIX, a TSG101- and CHMP4b-binding protein), have been found to be involved in membrane remodeling events that accompany endosomal protein sorting, cytokinesis, and the budding of several enveloped viruses, such as human immunodeficiency virus type 1 (HIV-1) [10–12]. The ESCRT complexes I, II, and III are sequentially, or perhaps concentrically recruited to the endosomal membrane to sequester

cargo proteins and drive vesicularization into the endosome. Finally, ESCRT-III recruits Vps4 (two isoforms, Vps4A and Vps4B), a member of the AAA-family of ATPase that disassembles and thereby terminates and recycles the ESCRT machinery.

Since HCV is also an enveloped RNA virus, we hypothesized that the ESCRT system might be required for HCV production. To test this hypothesis, we examined the release of HCV Core into culture supernatants from cells rendered defective for ESCRT components by RNA interference. The results provide evidence that the ESCRT system is required for HCV production.

Materials and Methods

Cell Culture

293FT cells (Invitrogen, Carlsbad, CA) were cultured in Dulbecco's modified Eagle's medium (DMEM; Invitrogen) supplemented with 10% fetal bovine serum (FBS). The HuH-7-derived cell line, RSc cured cells that cell culture-generated HCV-JFH1 (JFH1 strain of genotype 2a) [13] could infect and effectively replicate [14–16] and OR6c and OR6 cells harboring the genome-length HCV-O RNA with luciferase as a reporter were cultured in DMEM with 10% FBS as described previously [17,18].

Plasmid Construction

To construct pcDNA3-FLAG-Alix, a DNA fragment encoding Alix was amplified from total RNAs derived from RSc cells by RT-PCR using the follwing pairs of primers: Forward 5′-CGGG-ATCCAAGATGGCGACATTCATCTCGGT-3′ and reverse 5′-CCGGCGGCCGCTTACTGCTGTGGATAGTAAG-3′. The obtained DNA fragment was subcloned into *Bam*HI-*Not*I of pcDNA3-FLAG vector [19], and the nucleotide sequences were determined by Big Dye termination cycle sequencing using an ABI Prism 310 genetic analyzer (Applied Biosystems, Foster City, CA, USA). The plasmid of pJRN/3-5B was based on pJFH1 [13] and was constructed as previously described [20].

RNA synthesis, RNA transfection, and Selection of G418-resistant cells

Plasmid pJRN/3-5B were linearized by *Xba*I and used for the RNA synthesis with the T7 MEGAScript kit (Ambion, Austin, TX). *In vitro* transcribed RNA was transfected into OR6c cells by electroporation [17,18]. The transfected cells were selected in culture medium containing G418 (0.3 mg/ml) for 3 weeks. We referred to them as OR6c/JRN 3-5B cells.

Immunofluorescence and Confocal Microscopic Analysis

Cells were fixed in 3.6% formaldehyde in phosphate-buffered saline (PBS) and permeabilized in 0.1% Nonidet P-40 (NP-40) in PBS at room temperature as previously described [21]. Cells were incubated with anti-HCV Core antibody (CP-9 and CP-11 mixture; Institute of Immunology, Tokyo, Japan), anti-Myc-Tag antibody (PL14; Medical & Biological Laboratories, MBL, Nagoya, Japan), anti-Alix antibody (Covalab, Villeurbanne, France), and/or anti-FLAG polyclonal antibody (Sigma, St. Louis, MO) at a 1:300 dilution in PBS containing 3% bovine serum albumin (BSA) at 37°C for 30 min. Cells were then stained with fluorescein isothiocyanate (FITC)-conjugated anti-rabbit antibody (Jackson ImmunoResearch, West Grove, PA) or anti-Cy3-conjugated anti-mouse antibody (Jackson ImmunoResearch) at a 1:300 dilution in PBS containing BSA at 37°C for 30 min. Lipid droplets and nuclei were stained with BODIPY 493/503 (Molecular Probes, Invitrogen) and DAPI (4′,6′-diamidino-2-phenylindole), respectively. Following extensive washing in PBS, cells were mounted on slides using a mounting media of 90% glycerin/10% PBS with 0.01% *p*-phenylenediamine added to reduce fading. Samples were viewed under a confocal laser-scanning microscope (LSM510; Zeiss, Jena, Germany).

RNA Interference

The following siRNAs were used: human TSG101 (siGENOME SMARTpool M-003549-01-0005 and 5′-CCUCCAGU-CUUCUCUCGUCUU-3′ sense, 5′-GACGAGAGAAGACUG-GAGGUU-3′ antisense), human Alix/PDCD6IP (siGENOME SMARTpool M-004233-02-0005), human Vps4B (siGENOME SMARTpool M-013119-02-0005), human CHMP4b (siGENOME SMARTpool M-018075-00-0005), and siGENOME Non-Targeting siRNA Pool#1 (D-001206-13-05) (Dharmacon, Thermo Fisher Scientific, Waltham, MA) as a control. siRNAs (50 nM final concentration) were transiently transfected into either RSc cells [14–16] or OR6 cells [17,18] using Oligofectamine (Invitrogen) according to the manufacturer's instructions. Oligonucleotides with the following sense and antisense sequences were used for the cloning of short hairpin (sh) RNA-encoding sequences against TSG101, Alix, Vps4B, or CHMP4b in lentiviral vector: TSG101i, 5′-GATCCCC GGAGGAAATGGATCGTGCCTT-CAAGAGAGGCACGATCCATTTCCTCCTTTTTGGAAA-3′ (sense), 5′-AGCTTTTCCAAAAAGGAGGAAATGGATCGTG-CCTCTCTTGAAGGCACGATCCATTTCCTCCGGG-3′ (antisense); Alixi, 5′-GATCCCC GGAGGTGTTCCCTGTCTTG-TTCAAGAGACAAGACAGGGAACACCTCCTTTTTGGAA-A-3′ (sense), 5′-AGCTTTTCCAAAAAGGAGGTGTTCCCTG-TCTTGTCTCTTGAACAAGACAGGGAACACCTCCGGG-3′ (antisense); Vps4Bi, 5′-GATCCCC GGAGAATCTGATGATC-CTGTTCAAGAGACAGGATCATCAGATTCTCCTTTTTG-GAAA-3′ (sense), 5′-AGCTTTTCCAAAAAGGAGAATCT-GATGATCCTGTCTCTTGAACAGGATCATCAGATTCTC-CGGG-3′ (antisense); CHMP4bi, 5′-GATCCCC GAGGAG-GACGACGACATGATTCAAGAGATCATGTCGTCGTCC-TCCTCTTTTTGGAAA-3′ (sense), 5′-AGCTTTTCCAAAAA-GAGGAGGACGACGACATGATCTCTTGAATCATGTCG-TCGTCCTCCTCGGG-3′ (antisense); Broxi, 5′-GATCCCCG-GATGACAGTACTAAACCCTTCAAGAGAGGGTTTAGTA-CTGTCATCCTTTTTGGAAA-3′ (sense), 5′-AGCTTTTC-CAAAAAGGATGACAGTACTAAACCCTCTCTTGAAGGG-TTTAGTACTGTCATCCGGG-3′ (antisense). The oligonucleotides above were annealed and subcloned into the *Bgl*II-*Hin*dIII site, downstream from an RNA polymerase III promoter of pSUPER [22], to generate pSUPER-TSG101i, pSUPER-Alixi, pSUPER-Vps4Bi, and pSUPER-CHMP4bi, respectively. To construct pLV-TSG101i, pLV-Alixi, pLV-Vps4Bi, and pLV-CHMP4bi, the *Bam*HI-*Sal*I fragments of the corresponding pSUPER plasmids were subcloned into the *Bam*HI-*Sal*I site of pRDI292 [23], an HIV-1-derived self-inactivating lentiviral vector containing a puromycin resistant marker allowing for the selection of transduced cells, respectively.

Lentiviral Vector Production

The vesicular stomatitis virus (VSV)-G-pseudotyped HIV-1-based vector system has been described previously [24–26]. The lentiviral vector particles were produced by transient transfection of the second-generation packaging construct pCMV-ΔR8.91 [24–26] and the VSV-G-envelope-expressing plasmid pMDG2 as well as pRDI292 into 293FT cells with FuGene6 (Roche Diagnostics, Basel, Switzerland).

HCV Infection Experiments

The supernatants was collected from cell culture-generated HCV-JFH1 [13]-infected RSc cells [14–16] at 5 days post-

infection and stored at −80°C after filtering through a 0.45 μm filter (Kurabo, Osaka, Japan) until use. For infection experiments with HCV-JFH1 virus, RSc cells (1×10^5 cells/well) were plated onto 6-well plates and cultured for 24 hours (hrs). Then, we infected the cells with 50 μl (equivalent to a multiplicity of infection [MOI] of 0.1) of inoculum. The culture supernatants were collected and the levels of HCV Core were determined by enzyme-linked immunosorbent assay (ELISA) (Mitsubishi Kagaku Bio-Clinical Laboratories, Tokyo, Japan). Total RNA was isolated from the infected cellular lysates using RNeasy mini kit (Qiagen, Hilden, Germany) for quantitative RT-PCR analysis of intracellular HCV RNA. The infectivity of HCV in the culture supernatants was determined by a focus-forming assay at 48 hrs post-infection. The HCV infected cells were detected using anti-HCV Core antibody (CP-9 and CP-11). Intracellular HCV infectivity was determined by a focus-forming assay at 48 hrs post-inoculation of lysates by repeated freeze and thaw cycles (three times).

Quantitative RT-PCR Analysis

The quantitative RT-PCR analysis for HCV RNA was performed by real-time LightCycler PCR (Roche) as described previously [17,18]. We used the following forward and reverse primer sets for the real-time LightCycler PCR: TSG101, 5′-ATGGCGGTGTCGGAGAGCCA-3′ (forward), 5′-AACAGGTTTGAGATCTTTGT-3′ (reverse); Alix, 5′-ATGGCGACATTCATCTCGGT-3′ (forward), 5′-TACTGGGCCTGCTCTTCCCC-3′ (reverse); Vps4B, 5′-ATGTCATCCACTTCGCCCAA-3′ (forward), 5′-ATACTGCACAGCATGCTGAT-3′ (reverse); CHMP4b, 5′-ATGTCGGTGTTCGGGAAGCT-3′ (forward), 5′-ATCTCTTCCGTGTCCCGCAG-3′ (reverse); Brox, 5′-ATGACCCATTGGTTTCATAG-3′ (forward), 5′-CCTGGATGACCTCAAGTCAT-3′ (reverse); β-actin, 5′-TGACGGGGTCACCCACACTG-3′ (forward), 5′-AAGCTGTAGCCGCGCTCGGT-3′ (reverse); and HCV-JFH1, 5′-AGAGCCATAGTGGTCTGCGG-3′ (forward), 5′-CTTTCGCAACCCAACGCTAC-3′ (reverse).

MTT Assay

Cells (5×10^3 cells/well) were plated onto 96-well plates and cultured for 24, 48 or 72 hrs, then, subjected to the colorimetric 3-(4,5-dimethylthiazol-2-yl)-2,5-diphenyltetrazolium bromid (MTT) assay according to the manufacturer's instructions (Cell proliferation kit I, Roche). The absorbance was read using a microplate reader (Multiskan FC, Thermo Fisher Scientific) at 550 nm with a reference wavelength of 690 nm.

Renilla Luciferase (RL) Assay

OR6 cells (1.5×10^4 cells/well) [17,18] were plated onto 24-well plates and cultured for 24 hrs. The cells were transfected with siRNAs (50 nM) using Oligofectamine and incubated for 72 hrs, then, subjected to the RL assay according to the manufacturer's instructions (Promega, Madison, WI). A lumat LB9507 luminometer (Berthold, Bad Wildbad, Germany) was used to detect RL activity.

Western Blot Analysis

Cells (2×10^5 cells/well) were plated onto 6-well plates and cultured for 24 or 48 hrs. Cells were lysed in buffer containing 50 mM Tris-HCl (pH 8.0), 150 mM NaCl, 4 mM EDTA, 1% NP-40, 0.1% sodium dodecyl sulfate (SDS), 1 mM dithiothreitol (DTT) and 1 mM phenylmethylsulfonyl fluoride (PMSF). Supernatants from these lysates were subjected to SDS-polyacrylamide gel electrophoresis, followed by immunoblot analysis using anti-TSG101 antibody (BD Transduction Laboratories, San Jose, CA), anti-Alix antibody, anti-Vps4B antibody (Abnova, Taipei, Taiwan) (A302-078A; Bethyl Laboratories, Montgomery, TX), anti-CHMP4B antibody (sc-82557; Santa Cruz Biotechnology, Santa Cruz, CA), anti-HCV Core antibody, anti-β-actin antibody (Sigma), anti-Myc-Tag antibody, anti-FLAG antibody (M2; Sigma), anti-Chk2 antibody (DCS-273; MBL), anti-heat shock protein (HSP) 70 antibody (BD), Living Colors A.v. monoclonal antibody (JL-8; Clontech, Mountain View, CA), anti-HCV NS5A monoclonal antibody (no. 8926; a generous gift from A Takamizawa, The Research Foundation for Microbial Diseases of Osaka University, Japan), or anti-HCV NS5A polyclonal antibody (a generous gift from K Shimotohno, Chiba Institute of Technology, Chiba, Japan).

Immunoprecipitation Analysis

Cells were lysed in buffer containing 10 mM Tris-HCl (pH 8.0), 150 mM NaCl, 1% NP-40, 1 mM PMSF, and protease inhibitor cocktail containing 104 μM 4-(2-aminoethyl)benzenesulfonyl fluoride hydrochloride, 80 nM aprotinin, 2.1 μM leupeptin, 3.6 μM bestatin, 1.5 μM pepstatin A, and 1.4 μM E-64 (Sigma). Lysates were pre-cleaned with 30 μl of protein-G-Sepharose (GE Healthcare Bio-Sciences). Pre-cleaned supernatants were incubated with 5 μl of Living Colors A.v. monoclonal antibody or anti-FLAG antibody at 4°C for 1 hr. Following absorption of the precipitates on 30 μl of protein-G-Sepharose resin for 1 hr, the resin was washed four times with 700 μl lysis buffer. Proteins were eluted by boiling the resin for 5 min in 1× Laemmli sample buffer. The proteins were then subjected to SDS-PAGE, followed by immunoblotting analysis using either anti-FLAG antibody, Living Colors A.v. monoclonal antibody or anti-HCV Core antibody.

Statistical Analysis

Statistical comparison of the infectivity of HCV in the culture supernatants between the knockdown cells and the control cells was performed using the Student's *t*-test. *P* values of less than 0.05 were considered statistically significant. All error bars indicate standard deviation.

Results

The ESCRT system is required for HCV production

To investigate the potential role(s) of the ESCRT system in the HCV life cycle, we first used lentiviral vector-mediated RNA interference to stably knockdown the ESCRT components, including TSG101, Alix, Vps4B, or CHMP4b in HuH-7-derived RSc cured cells that cell-culture-generated HCVcc (HCV-JFH1, genotype 2a) [13] could infect and effectively replicate [14–16]. We used puromycin-resistant pooled cells 10 days after the lentiviral transduction in all experiments. Western blot and real-time LightCycler RT-PCR analyses for TSG101, Alix, Vps4B, or CHMP4b demonstrated a very effective knockdown of each ESCRT component in RSc cells transduced with lentiviral vectors expressing the corresponding shRNAs (Fig. 1A–E). Importantly, we noticed that the depletion of ESCRT components did not affect the levels of several cellular proteins, including HSP70, Chk2, and b-actin (Fig. 1A). To test the cell toxicity of each shRNA, we examined colorimetric MTT assay. In this context, we demonstrated that the shRNAs did not affect the cell viabilities (Fig. 1F). We next examined the levels of HCV Core and the infectivity of HCV in the culture supernatants as well as the level of HCV RNA in the TSG101, Alix, Vps4B, or CHMP4b stable knockdown RSc cells 97 h after HCV-JFH1 infection at an MOI of 0.1. The results showed that the release of HCV Core into the culture supernatants

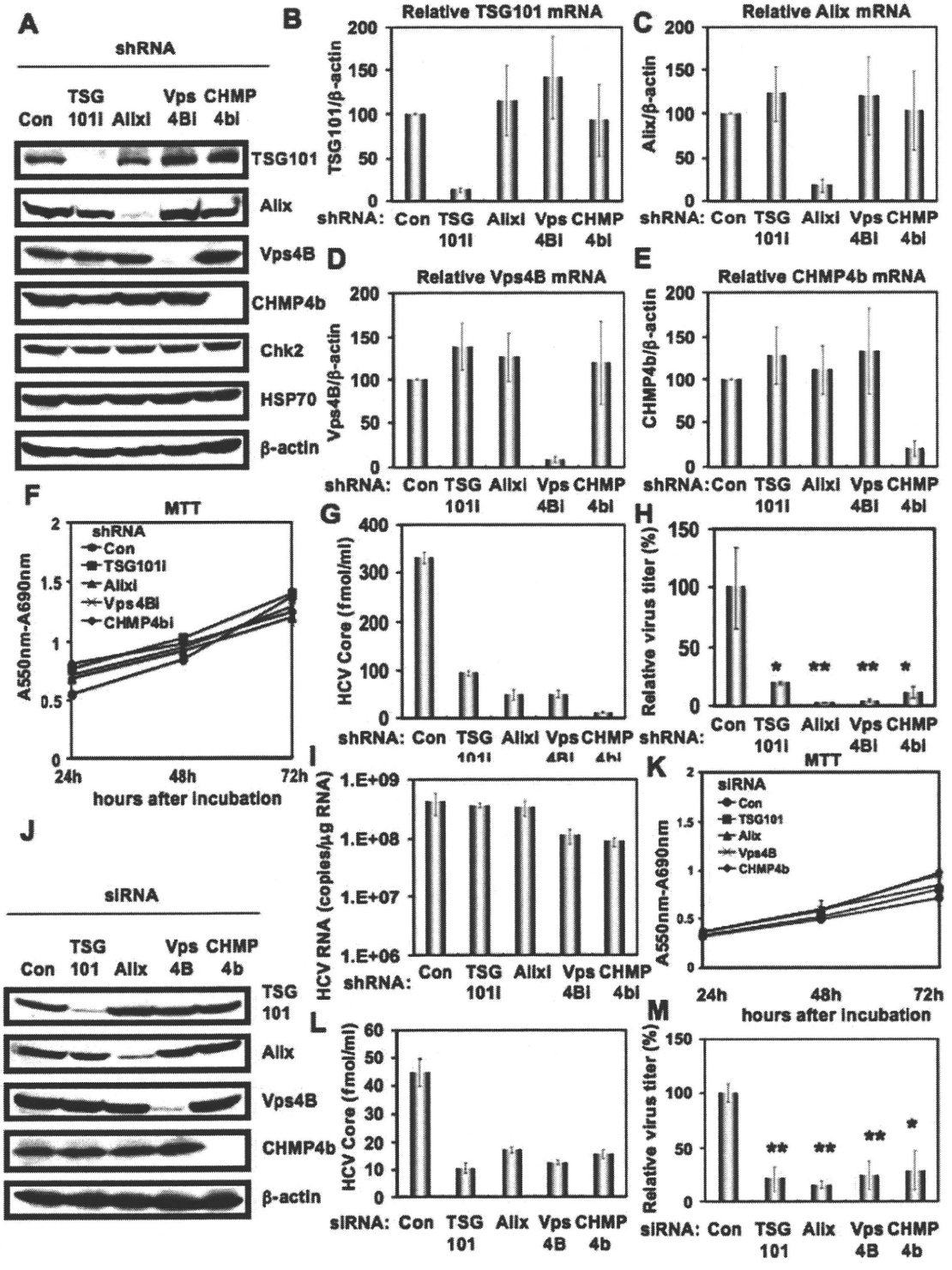

Figure 1. ESCRT components are required for the infectious HCV production. (A) Inhibition of TSG101, Alix, Vps4B, or CHMP4b protein expression by shRNA-producing lentiviral vectors. The results of the Western blot analysis of cellular lysates with anti-TSG101, anti-Alix, anti-Vps4B, anti-CHMP4b, anti-Chk2, anti-HSP70, or anti-β-actin antibody in RSc cells expressing shRNA targeted to TSG101 (TSG101i), Alix (Alixi), Vps4B (Vps4Bi), or CHMP4b (CHMP4bi) as well as in RSc cells transduced with a control lentiviral vector (Con) are shown. Real-time LightCycler RT-PCR for TSG101 (B), Alix (C), Vps4B (D), or CHMP4b mRNA (E) was performed as well as for β-actin mRNA in triplicate. Each mRNA level was calculated relative to the level in RSc cells transduced with a control lentiviral vector (Con) which was assigned as 100%. Error bars in this panel and other figures indicate standard deviations. (F) MTT assay of each knockdown RSc cells at the indicated time. (G) The levels of HCV Core in the culture supernatants from the stable knockdown RSc cells 97 h after inoculation of HCV-JFH1 at an MOI of 0.1 were determined by ELISA. Experiments were done in triplicate and columns represent the mean Core protein levels. (H) The infectivity of HCV in the culture supernatants from the stable knockdown RSc cells 97 hrs after inoculation of HCV-JFH1 at an MOI of 0.1 was determined by a focus-forming assay at 48 hrs post-infection. Experiments were done in triplicate and each virus titer was calculated relative to the level in RSc cells transduced with a control lentiviral vector (Con) which was assigned as 100%. Asterisks indicate significant differences compared to the control treatment. *$P<0.05$; **$P<0.01$. (I) The level of intracellular genome-length HCV-JFH1 RNA in the cells at 97 hrs post-infection was monitored by real-time LightCycler RT-PCR. Results

from three independent experiments are shown. (J) Inhibition of TSG101, Alix, Vps4B, or CHMP4b protein expression by 72 hrs after transient transfection of RSc cells with a pool of control siRNA (Con) or a pool of siRNA specific for Alix, Vps4B, or CHMP4b (50 nM). The results of the Western blot analysis of cellular lysates with anti-TSG101, anti-Alix, anti-Vps4B, anti-CHMP4b, or anti-β-actin antibody is shown. (K) MTT assay of each knockdown RSc cells at the indicated time. (L) The levels of HCV Core in the culture supernatants were determined by ELISA 24 hrs after inoculation of HCV-JFH1. RSc cells were transiently transfected with a pool of control siRNA (Con) or a pool of siRNA specific for TSG101, Alix, Vps4B, or CHMP4b (50 nM). At 48 hrs after transfection, the cells were inoculated with HCV-JFH1 at an MOI of 5 and incubated for 2 hrs. Then, culture medium was changed and incubated for 22 hrs. Experiments were done in triplicate and each Core level was calculated relative to the level in the culture supernatants from the control cells and indicated below. (M) The infectivity of HCV in the culture supernatants from the transient knockdown RSc cells 24 hrs after inoculation of HCV-JFH1 at an MOI of 5 was determined by a focus-forming assay at 48 hrs post-infection. Experiments were done in triplicate and each virus titer was calculated relative to the level in RSc cells transfected with a control siRNA (Con) which was assigned as 100%. Asterisks indicate significant differences compared to the control treatment. *$P<0.05$; **$P<0.01$.

doi:10.1371/journal.pone.0014517.g001

was significantly suppressed in these knockdown cells after HCV-JFH1 infection (Fig. 1G). Importantly, the infectivity of HCV in the culture supernatants was also significantly suppressed in these knockdown cells (Fig. 1H), while the RNA replication of HCV-JFH1 was not affected in the TSG101 or Alix knockdown cells and was somewhat decreased in the Vps4B and CHMP4b knockdown cells (Fig. 1I). This suggested that the ESCRT system is associated with infectious HCV production. To further confirm whether or not the ESCRT system is involved in HCV production, we analyzed the single-round HCV replication. For this, we used RSc cells transiently transfected with a pool of siRNAs specific for TSG101, Alix, Vps4B, or CHMP4b as well as a pool of control siRNAs (Con) following HCV infection. In spite of very effective knockdown of each ESCRT component (Fig. 1J), we demonstrated that the siRNAs did not affect the cell viabilities by MTT assay (Fig. 1K). Consistent with our finding using the stable knockdown cells, we observed that the release of HCV Core or the infectivity of HCV into the culture supernatants was significantly suppressed in these transient knockdown cells 24 hrs after HCV-JFH1 infection (Fig. 1L and 1M). Furthermore, we examined the effect of siRNA specific for TSG101, Alix, Vps4B, or CHMP4b in HCV RNA replication using the subgenomic JFH1 replicon, JRN/3-5B, encoding *Renilla* luciferase gene for monitoring the HCV RNA replication in HuH-7-derived OR6c JRN/3-5B cells (Fig. 2A and 2B) or an OR6 assay system, which was developed as a luciferase reporter assay system for monitoring genome-length HCV RNA replication (HCV-O, genotype 1b) in HuH-7-derived OR6 cells (Fig. 2C) [17,18]. The results showed that these siRNAs could not affect HCV RNA replication as well as the levels of intracellular NS5A proteins (Fig. 2A–C). Although we have demonstrated that the ESCRT system is required for production of extracellular infectious HCV particles, it is not clear whether or not these findings are associated with the assembly of intracellular infectious particles. To test this point, infectivity of intracellular infectious particles was analyzed following lysis of HCV-JFH1-infected knockdown cells by repetitive freeze and thaw. Consequently, we did not observe any significant effects of siRNAs on the accumulation of intracellular infectious HCV-JFH1, while the accumulation of extracellular HCV was significantly suppressed in these knockdown cells (Fig. 2D and 2E), indicating that inhibition of the ESCRT system does not block the accumulation of intracellular infectious HCV particles. Furthermore, Western blot analysis of cell lysates demonstrated that the level of intracellular HCV Core and NS5A was not affected in these knockdown cells 72 hrs post-infection (Fig. 2F). Thus, we conclude that the ESCRT system is not required for the assembly of infectious particles but the ESCRT system is required for late step of HCV production.

HCV Core can target into lipid droplets in the ESCRT knockdown cells

Since lipid droplets have been shown to be involved in an important cytoplasmic organelle for HCV production [4], we performed immunofluorescence and confocal microscopic analyses to determine whether or not HCV Core misses localization into lipid droplets in the ESCRT knockdown cells. We found that the Core was targeted into lipid droplets even in TSG101 knockdown, Alix knockdown, Vps4B knockdown, or CHMP4b knockdown RSc cells as well as in the control RSc cells after HCV infection (Fig. 3). This suggests that the ESCRT system plays a role in the late step after the Core is targeted into lipid droplets in the HCV life cycle.

HCV Core interacts with CHMP4b

To determine whether or not HCV Core can interact with ESCRT component(s), we examined their subcellular localization by confocal laser scanning microscopy. Consequently, the Core mostly colocalized with CHMP4b-green fluorescent protein (GFP) or FLAG-tagged CHMP4b in the perinuclear region of 293FT cells coexpressing them (Fig. 4A and 4B), while the CHMP4b-GFP alone was slightly diffused in the cytoplasm (Fig. 4A), indicating the recruitment of CHMP4b in the Core-expressing area. Importantly, we observed similar partial colocalization in HCV-JFH1-infected RSc cells expressing CHMP4b-GFP (Fig. 4C), whereas the CHMP4b-GFP alone was diffused in the cytoplasm in the uninfected RSc cells (Fig. 4C), suggesting the interaction of HCV Core with CHMP4b. Unfortunately, we failed to observe endogenous CHMP4b using several commercially available anti-CHMP4b antibody (data not shown). Consistent with a previous report that interaction between HCV Core and NS5A is critical for HCV production [3], we found the partial colocalization of NS5A with CHMP4b-GFP as well as the colocalization of Core with CHMP4b-GFP in HCV-JFH1-infected RSc cells (Fig. 4C). Then, we examined whether or not HCV Core can bind to CHMP4b by immunoprecipitation analysis. 293FT cells transfected with 4 mg of pCHMP4b-GFP, pEGFP C3 (Clontech), pcDNA3-FLAG [19], pcDNA3-FLAG-Alix or pFLAG-CHMP4b and RSc cells 5 days after inoculation of HCV-JFH1 at an MOI of 4 were lysed and performed immunoprecipitation of lysate mixtures of HCV-JFH1-infected RSc cells and 293FT cells expressing CHMP4b-GFP, GFP alone, FLAG-CHMP4b or FLAG-epitope alone with anti-FLAG or anti-GFP antibody. Consequently, we observed that the Core but not the NS5A could bind to FLAG-CHMP4b (Fig. 4D). However, the Core was not immunoprecipitated with anti-FLAG antibody using the lysate mixtures of HCV-JFH1-infected RSc cell lysates and 293FT cells expressing FLAG-epitope alone or FLAG-Alix (Fig. 4D). Furthermore, the Core was coimmunoprecipitated with CHMP4b-GFP but not GFP when lysate mixtures of HCV-JFH1-infected RSc cells and 293FT cells expressing CHMP4b-GFP or GFP alone were used (Fig. 4D). In contrast, we failed to observe the marked colocalization of HCV-JFH1 Core with Myc-tagged TSG101 in HCV-JFH1-infected RSc cells expressing Myc-TSG101 or endogenous Alix in HCV-JFH1-infected RSc cells (Fig. 5A). Thus, we concluded that the HCV Core was associated with CHMP4b.

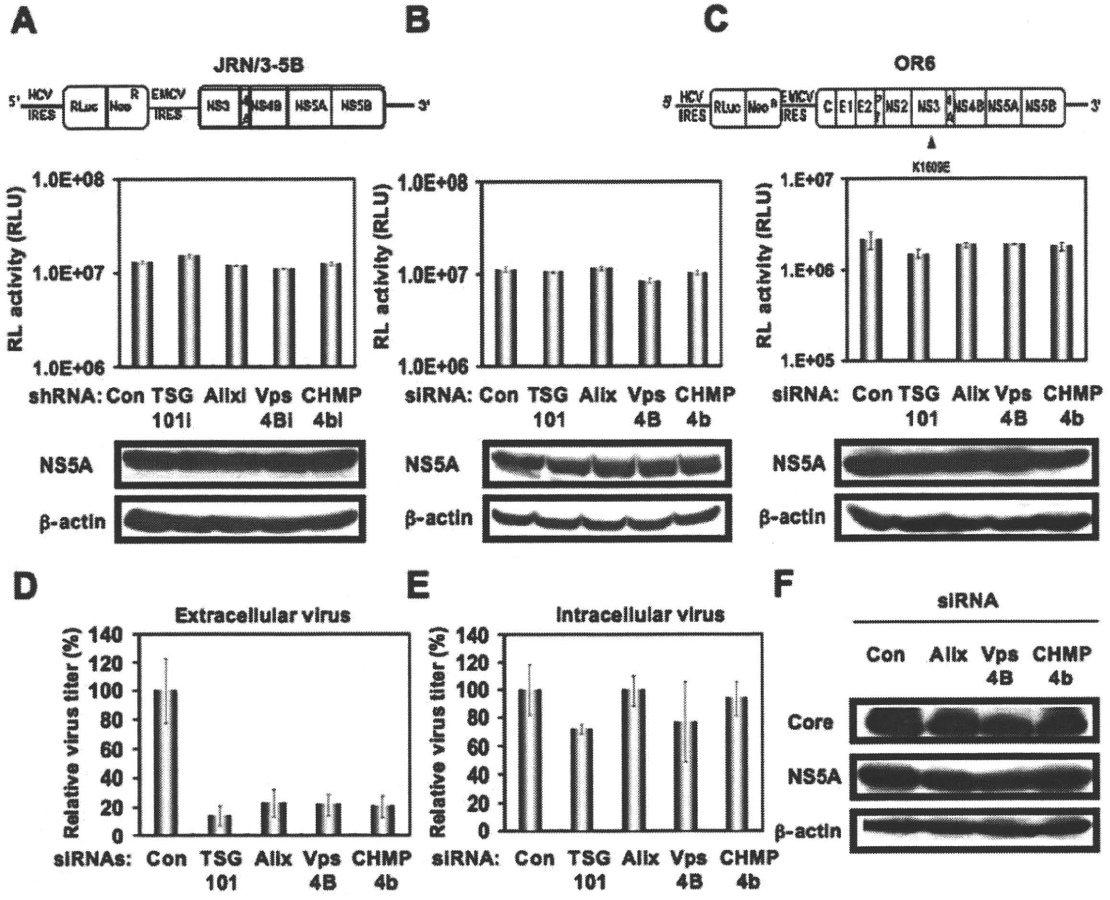

Figure 2. ESCRT system is not required for HCV RNA replication and assembly of intracellular infectious HCV. (A) Schematic gene organization of subgenomic JFH1 (JRN/3-5B) RNA encoding *Renilla* luciferase gene. Renilla luciferase gene (RLuc) is depicted as a box and is expressed as a fusion protein with Neo. The HCV RNA replication level in each ESCRT knockdown OR6c JRN/3-5B cells by lentiviral vector-mediated RNA interference (shRNA) was monitored by RL assay. The RL activity (RLU) is shown. The results shown are means from three independent experiments. (B) 72 hrs after the transfection of OR6c JRN/3-5B polyclonal cells with each of the siRNA (50 nM), the HCV RNA replication level was monitored by RL assay as described in (A). (C) Schematic gene organization of genome-length HCV-O RNA encoding *Renilla* luciferase gene. The position of an adaptive mutation, K1609E, is indicated by a triangle. 72 hrs after the transfection of OR6 cells with each of the siRNA (50 nM), the HCV RNA replication level was monitored by RL assay as described in (A). (D) The infectivity of HCV in the culture supernatants from the transient knockdown RSc cells 24 hrs after inoculation of HCV-JFH1 at an MOI of 2 was determined by a focus-forming assay at 48 hrs post-infection. Experiments were done in triplicate and each virus titer was calculated relative to the level in RSc cells transfected with a control siRNA (Con) which was assigned as 100%. (E) Intracellular HCV infectivity was determined by a focus-forming assay at 48 hrs post-inoculation of lysates by repeated freeze and thaw cycles as described in (D). (F) RSc cells were transiently transfected with a pool of control siRNA (Con) or a pool of siRNA specific for Alix, Vps4B, or CHMP4b (50 nM). At 24 hrs after the transfection, the cells were inoculated with HCV-JFH1 at an MOI of 0.2 and incubated for 48 hrs. Then, culture medium was changed and incubated for 24 hours. Western blotting of cell lysates 72 hrs post-infection with anti-β-actin, anti-HCV NS5A, or anti-HCV Core antibody is shown.
doi:10.1371/journal.pone.0014517.g002

Finally, we examined the subcellular localization of HCV Core and Brox, a novel farnesylated Bro1 domain-containing protein, since Brox was recently identified as a CHMP4-binding protein [27]. In this context, the Core partially colocalized with GFP-Brox in 293FT cells coexpressing of HCV Core and GFP-Brox (Fig. 5B). Importantly, we observed similar partial colocalization in HCV-JFH1-infected RSc cells expressing GFP-Brox (Fig. 5C). On the other hand, the CHMP4b-GFP alone was diffused in the cytoplasm of uninfected RSc cells (Fig. 5C). To examine the potential role of Brox in HCV life cycle, we established the Brox knockdown RSc cells by lentiviral vector expressing shRNA targeted to Brox (Fig. 5D). Consequently, we found that the release of HCV Core or the infectivity of HCV into the culture supernatants was significantly suppressed in the Brox knockdown cells 4 days after HCV-JFH1 infection (Fig. 5E and 5F), while the RNA replication of HCV-JFH1 was marginally affected in the knockdown cells (Fig. 5G) in spite of the very effective knockdown of Brox mRNA (Fig. 5D), suggesting that Brox is also required for the infectious HCV production.

Discussion

In this study, we have demonstrated that the ESCRT system is required for infectious HCV production, and that HCV Core but not NS5A binds to CHMP4b, a component of ESCRT-III. Although RNA replication of HCV-JFH1 was not affected in the TSG101 knockdown or the Alix knockdown cells, the infectivity of HCV in the culture supernatants was significantly suppressed in these knockdown cells after HCV-JFH1 infection (Fig. 1G and 1H). Furthermore, siRNA targeted to TSG101, Alix, Vps4B, or CHMP4b significantly suppressed HCV Core level or the infectivity of HCV in the culture supernatants (Fig. 1L, 1M, and